Progress in Organic Coatings 137 (2019) 105373

Contents lists available at ScienceDirect

Progress in Organic Coatings

journal homepage: www.elsevier.com/locate/porgcoat

Review

Recent developments in air-trapped superhydrophobic and liquid-infused slippery surfaces for anti-icing application

Sanjay S. Latthe[a,b], Rajaram S. Sutar[b], Appasaheb K. Bhosale[b], Saravanan Nagappan[c], Chang-Sik Ha[c], Kishor Kumar Sadasivuni[d], Shanhu Liu[a,*], Ruimin Xing[a,*]

[a] Henan Key Laboratory of Polyoxometalate Chemistry, Henan Joint International Research Laboratory of Environmental Pollution Control Materials, College of Chemistry and Chemical Engineering, Henan University, Kaifeng, 475004, PR China
[b] Self-cleaning Research Laboratory, Department of Physics, Raje Ramrao College, Jath 416404, Affiliated to Shivaji University, Kolhapur, Maharashtra, India
[c] Department of Polymer Science and Engineering, Pusan National University, Busan 46241, Republic of Korea
[d] Center for Advanced Materials, Qatar University, P. O. Box 2713, Doha, Qatar

ARTICLE INFO

Keywords:
Anti-icing
Superhydrophobic
Wettability
SLIPS
Freezing
Lotus leaf

ABSTRACT

Anti-icing coating is one of the recent hot topics in industrial applications as well as from the academic viewpoint. Icing is one of the major problem on various substrates such as glass windows in buildings as well as vehicles, solar panels, wind turbine blades, airplanes, transmission lines, power towers, traffic signals, off-shore oil platforms, telecommunication antennas, and many others. Ice accumulation can significantly reduce the performance of the substrates and results in poor visibility. Recently, considerable attention is being paid on the naturally inspired superhydrophobic/icephobic surfaces by mimicking its surface property for the development of artificial self-cleaning superhydrophobic and ice-phobic surfaces. A good example is the lotus leaf surface where hierarchical micro and nano-scale rough structure covered by low surface energy coating layer on the leaf can repel water droplets and prevent ice accumulation. On superhydrophobic surfaces, impacting and condensed water droplets rolled off before freezing at subzero temperature. On the other hand, in slippery liquid-infused porous surface (SLIPS), the air pockets are replaced by immiscible lubricant film which can easily remove the accumulated ice without any damage to the surface. In this review article, we describe the recent progress in passive anti-icing coating materials and methodologies. Metal substrates, polymers, and nanoparticles/polymer composites are playing the major role in the development of anti-icing surface. So, the main goal of this review articles deals with the development of various synthetic routes of superhydrophobic anti-icing coating materials from metal substrates, polymers, and nanoparticles/polymer composites. In addition, the role of SLIPS in anti-icing coating and their use are also discussed.

1. Introduction

Superhydrophobic and anti-icing surfaces are essential for saving energy and economy in industrial, transportation, and icing applications [1–4]. In nature, a lotus-leaf repels water droplets due to the presence of micro-nano hierarchical surface with micro-size papillae covered by a thin layer of nano-wax crystals. The small radius of the tip of papillae minimizes the contact area of water drops [5,6]. Owing to the very low sliding angle behavior of superhydrophobic surfaces, the ball-shaped water rolls off by collecting dust and ultimately clean the surface. This phenomenon is known as lotus effect or self-cleaning effect [6–8]. The wettability (especially, hydro-affinity) of a solid surface can be defined in terms of water contact angle (WCA) and surface roughness. Fig. 1 depicts the variation in contact angles on different solid surfaces depending on surface structure and surface energy [9]. Normally, a hydrophilic surface is smooth and show high wettability with low WCA ($\theta < 90^{\circ}$), while a hydrophobic surface shows partial wettability and greater WCA ($\theta > 90^{\circ}$). On the other hand, superhydrophobic surface completely repel water droplets because of zero wettability and very high WCA ($\theta > 150^{\circ}$) [10]. In Wenzel's type regime [11], water droplets penetrate into the rough cavity of the surface, cannot roll off, and remain pinned. However, in the case of the Cassie-Baxter's type model [12], air infuse into the rough surface which significantly reduces the contact area of liquid and solid surface; and hence, the water droplets easily roll off.

The Cassie-Baxter's type non-wetting property of the lotus leaf has

* Corresponding authors.
E-mail addresses: liushanhu@vip.henu.edu.cn (S. Liu), rmxing@henu.edu.cn (R. Xing).

https://doi.org/10.1016/j.porgcoat.2019.105373
Received 25 July 2019; Received in revised form 18 September 2019; Accepted 25 September 2019

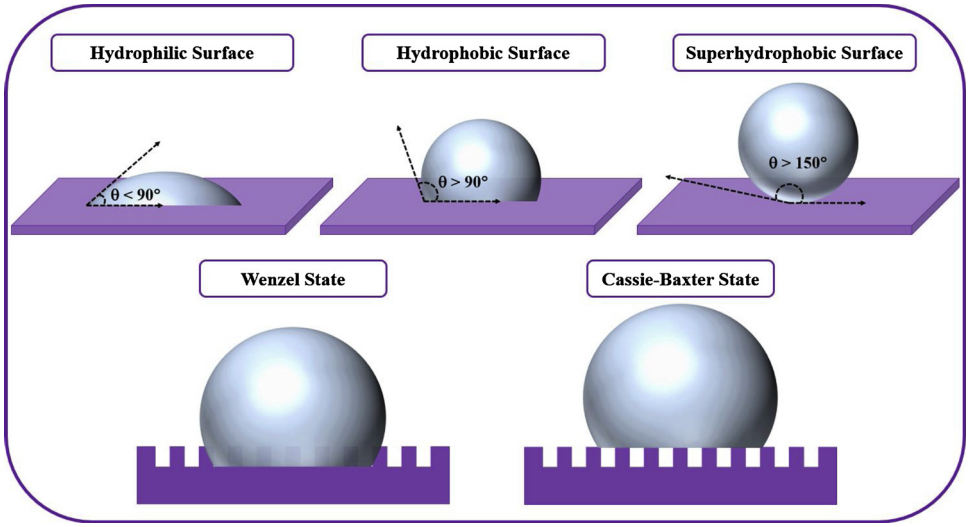

Fig. 1. The shape of water drops on different type of surfaces.

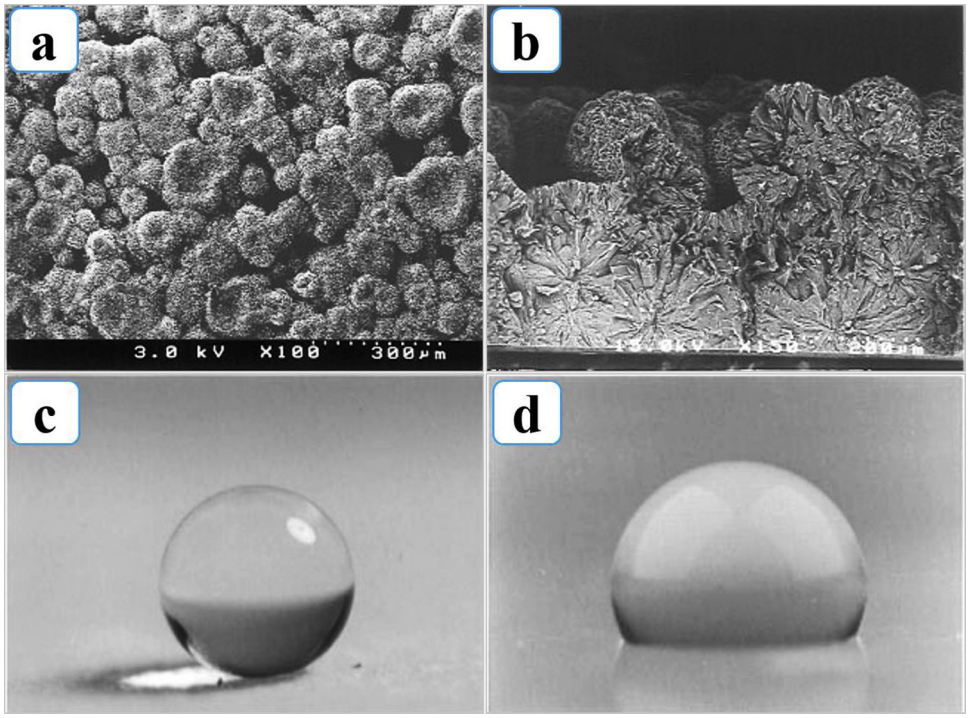

Fig. 2. SEM images of the fractal AKD surface: (a) top and (b) cross sectional view. Photographs of a water droplet on (c) fractal AKD surface (θ = 174°) and flat AKD surface (θ = 109°). Reproduced from ref. [13] with permission from American Chemical Society, Copyright 1996.

inspired many researchers to fabricate self-cleaning superhydrophobic surfaces from lab to industrial scales. The first attempt to prepare artificial superhydrophobic surface was made by Onda and his research team [13]. They have prepared fractal-like superhydrophobic film by immersing a glass plate in melted alkylketene dimer (AKD) followed-up with cooling, which exhibited excellent water repellency. According to the morphology and wettability analysis as shown in Fig. 2(a–d), a polymer grows into fractal shape after solidification and exhibits WCA of 174° as compared to flat AKD surface (WCA ~109°). Subsequently, Barthlott et al [6] confirmed that the superhydrophobicity of lotus leaf is due to the hierarchical micro/nanostructure of micropapillae and low surface energy wax nanorods. These two pioneer research articles of Onda and Barthlott have accelerated the research on developing smart superhydrophobic surfaces. Subsequently, many research articles were published, explaining the fabrication of superhydrophobic surfaces by merely controlling the surface micro/nanostructure and surface energy [14–18].

At present, the superhydrophobic surfaces are not just limited to self-cleaning application, they are also used in anti-icing and other smart applications [19]. The micro/nanoscale air pockets trapped in the hierarchical structure of superhydrophobic surface acts as a thermal barrier to cut-off the heat transfer during the icing process and, hence, effectively reduce the ice adhesion capacity [20]. Consequently, the ice could easily slide off the superhydrophobic surface. The effect of surface roughness and energy of the fabricated substrate plays a key role in the generation of superhydrophobic property and is obviously used for the prevention of ice accumulation on the substrate [21,22]. Wu et al. [21] studied the role of surface topography when the superhydrophobic surface showed icephobic property. They described that the presence of low surface materials on the prepared sol-gel composite materials

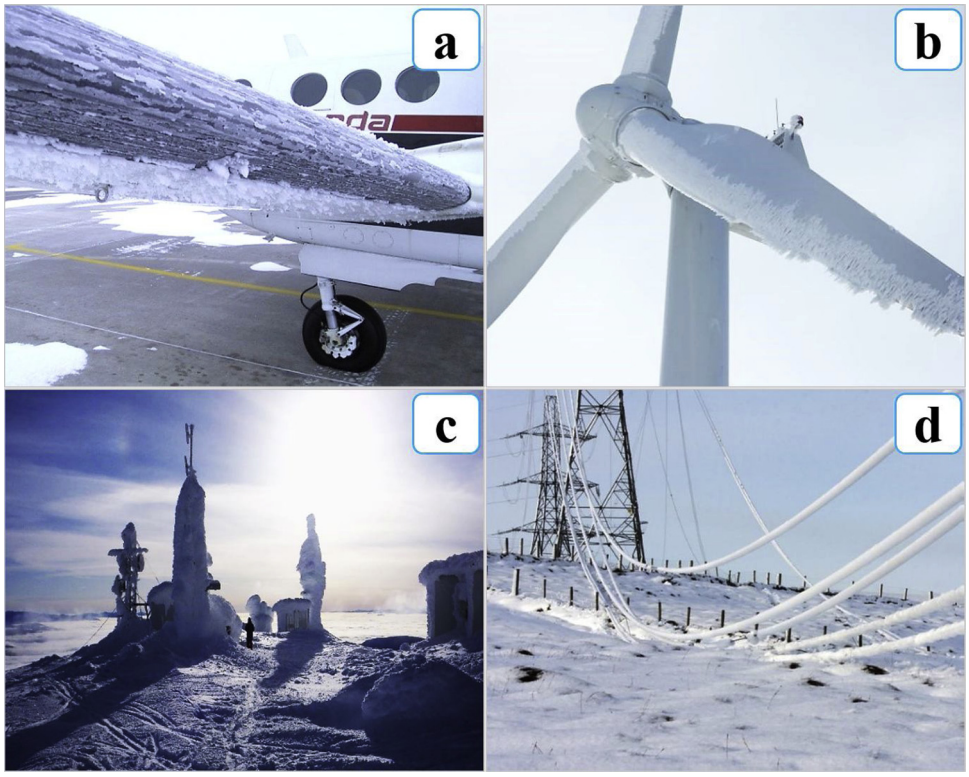

Fig. 3. Icing on a) an airplane b) wind turbines c) communication towers, and d) transmission lines. Reproduced from https://en.uit.no/forskning/forskningsgrupper/gruppe?p_document_id = 592,059.

showed better anti-icing behavior and low ice adhesion due to the presence of higher surface roughness and low surface energy materials. On the other hand, this might depend on the particular compositions of low surface material with other materials. Wu et al. [21] developed five different compositions of surfaces by increasing the content of low surface energy fluorinated silica nanoparticles with unmodified silica nanoparticles and functional silica sol. The results suggested that the higher content of low surface energy fluorinated silica nanoparticles in the composition would show high surface roughness (around 500 nm) and lower ice adhesion. The results clearly demonstrated the importance of higher surface roughness and lower surface energy materials in developing superhydrophobic surface property for anti-icing application. Ensikat et al. [22] used a Cryo-scanning electron microscopy (Cyro-SEM) to analyze the contact area between a droplet and superhydrophobic surface (liquid-solid interface). This technique is useful for analyzing the surface topography on the liquid-solid interface.

Nosonovsky et al. [23] studied the role of mechanical forces needed to detach a piece of ice, based on the receding contact angle of the superhydrophobic surface. Superhydrophobic surfaces possess lower shear strength due to higher contact angle. The formation of a small crack by the detachment of an ice piece on the superhydrophobic surface would lead to an increase in the shear force, which reduced the anti-icing property. The lower receding contact angle occasionally shows more ice adhesion as compared to higher receding contact angle. However, the results demonstrated that superhydrophobic surfaces did not always exhibit anti-icing behavior. Few studies also suggested that superhydrophobic coating delays ice accumulation on the surface as compared to the other coating surfaces. Wang et al. [24] developed a flexible superhydrophobic surface with robust anti-icing performance using poly(dimethylsiloxane) (PDMS) and zinc oxide (ZnO). This micro-nano hierarchical surface morphology was prepared by using soft lithography and hydrothermal deposition followed by the surface medication of the substrate with heptadecafluorodecyl tri-propoxy silane (FAS-17). This material effectively removed the deposited ice particles from the substrate within 30 s by 50 Hz horizontal vibration. Some authors have also prepared other types of durable superhydrophobic materials for anti-icing applications [25,26].

Various review articles have been published covering the mechanism of ice nucleation, frost formation, adhesion of ice following freezing, controlling ice formation, slippery surfaces for anti-icing, anti-icing and de-icing technologies, and applications [27–36]. In our review, we have exclusively focused on the importance of metal substrates, polymers, and nanoparticles/polymer composites for anti-icing coating and updated the recent progress on this topic. We believe that this review will provide a comprehensive outlook in the field of anti-icing applications.

2. Icing issues

Typically, various liquid/solid form of water can form in the cold environment. Frost, glaze, rime, snow, and ice forms of water can be formed from vapor or liquid form of water under different conditions. Frost nucleates from the vapor phase via de-sublimation or condensation with subsequent freezing, whereas the glaze is clear, dense, and rigid ice which forms from freezing rain of large droplets that are a few millimeters in diameter [37]. Rime is a milky, brittle, and feather-like ice that is formed from freezing of supercooled droplets [37]. Snow is a combination of ice and water, whereas ice is a brittle frozen state of water. In winter seasons, freezing rain storms crumble the power lines and communication towers. This results in electricity interruptions, including shutdown of water and heating facilities in residential and businesses areas. Hundreds of millions of dollars are spent after a severe storm to repair the damages. Typical examples are the Ice Storm'98 of Montreal and other eastern parts of Canada [38] and the severe snow storm that hit South China in 2008 [39]. In addition, icing results in major obstacles affecting the efficient use of renewable energy such as wind and solar energy [40,41], as well as aircraft icing [42], off-shore

oil platforms [43], snow and ice on roofs, bursting of water pipelines [44], car windows [45], and transmission lines [46]. In a humid environment, frost developed on solid surfaces may need heating for defrosting, which results in additional energy consumption [47]. Examples of major icing problems in aircraft, wind turbines, communication towers, and transmission lines are depicted in Fig. 3. To remove accumulated ice from solid surfaces is a challenging research. Current techniques for ice removal involves physical and chemical methods which are expensive and time consuming. Hence, the most effective way is to inhibit ice formation on solid surfaces rather than adopting expensive deicing processes. In recent years, anti-icing coating field is tremendously advancing by mimicking the naturally occurring materials such as the hydrophobic coatings in lotus.

3. Development of superhydrophobic/anti-icing surfaces

In nature, many biological surfaces such as plant leaves, insects, and bird wings exhibit superhydrophobic and anti-icing properties. The lotus leaf surface is well-known for its extreme water repellency and self-cleaning abilities. The hierarchical multiple rough structures on insects' wing surfaces are responsible for their extreme superhydrophobicity [48]. Ice adhesion on penguin's body is rarely observed, and they thermally insulate their body against cold seawater. Wang et al. [49] analyzed the surface structure of a penguin's feather and found that a penguin's feather was the best example for anti-frosting or anti-icing properties due to their air-infused micro/nanoscale hierarchical rough structures. The supercooled microdroplets of water on penguin's feather could achieve contact angle in nearly superhydrophobic state and revealed excellent anti-adhesion behavior. The penguin's body feathers are composed of two pinnae separated by the rachis (Fig. 4a). The pinnae contained fibrous barb (length ~5–7 mm and diameter ~25–30 μm) which are arranged parallel to the rachis (Fig. 4b1). The barb contained barbules (length ~300 μm and diameter ~7 μm) with numerous hamuli (diameter ~3 μm) found on the barbules (Fig. 4b2). The wrinkles morphology was observed on both barbules and hamuli (Fig. 4b3). Few hamuli were detected on the tips of the barbs (Fig. 4c1); nearly 100 nm deep grooves oriented along the barbs were also observed (Fig. 4c2). Such a micro/nanoscale hierarchical structure of penguin feather exhibited an WCA of around 147° (Fig. 4d), which effectively reduced water adhesion on the surface. Moreover, the authors simulated the microstructure of penguin's feather by fabricating the polyimide nanofiber membrane using electrospinning technique. The coalescence of the droplets on the membrane was effectively prevented by increasing the spacing between adjacent nanofibers, and hence, the membrane exhibited the anti-icing property.

Sun et al. [37] proposed that the poison dart frog skin can show better anti-icing behavior with stimuli-responsive nature by secreting mucus and toxins in their skin. Poison dart frog skin might have permeable superhydrophobic epidermis which isolate antifreeze-infused superhydrophilic dermis from the environment preventing glaze formation. Moreover, the growth of frost and rime on the surface of poison dart frog skin is removed by an antifreeze liquid through the epidermis. Another interesting example of anti-adhesive surface in nature is Nepenthes pitcher plants. In these plants, the ants and small insects slip and slide from the peristome surface and eventually fall into the digestive fluid inside the pitchers [50]. The trapping of prey using a slippery surface by Nepenthes pitcher plants has inspired the researchers to develop a new class of ice repellent surface called slippery liquid-infused porous surfaces (SLIPS). SLIPS are fabricated by infusing a lubricating liquid into a low surface energy micro/nanoporous solid surfaces which effectively reduces the contact angle hysteresis and pinning of water droplets [51–54].

Various polymer, polymer-nanoparticle composite and SLIPS-based surfaces are utilized for anti-icing applications. Saito and co-researchers [55] have first studied the ice and snow adhesion behavior on the rough superhydrophobic surface. Different mixtures of polytetrafluroethylene (PTFE) particles in polyvinylidene fluoride (PVDF) resin were spray-coated on plastic substrates. PTFE content of more than 60% in the coating resulted in superhydrophobicity with low surface free energy and anti-icing property. Koivuluoto et al [56] adopted flame-spray technique to deposit polyethylene (PE)-based polymer coating on metals for low ice adhesion. Dou et al. [57] spin-coated aqueous polyurethane lubricating layer on various substrates which showed reduced ice adhesion even at temperatures below −53 °C with repeated icing and de-icing cycles. Further, Xu et al [58] coated silicone–acrylate resin on small-scale wind turbine blades by dip and spray methods and confirmed that the highly hydrophobic surface provided better anti-icing ability. Inspired from micro-nanostructure of butterfly wings, Guo et al [59] developed micro-scaled ratchet structure (height ~80 μm) on

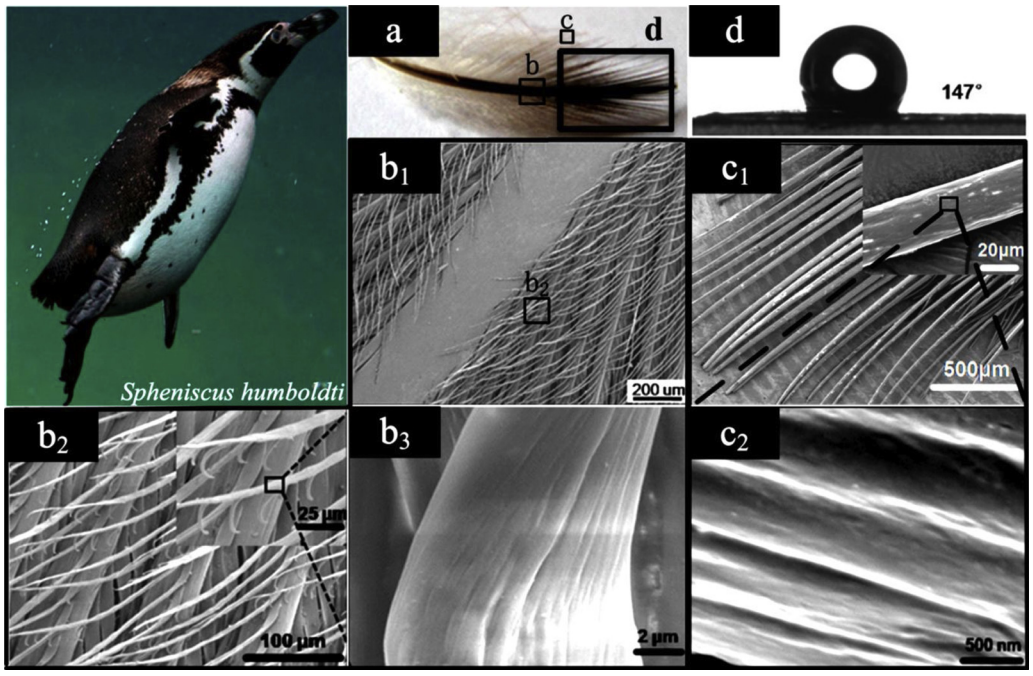

Fig. 4. (a) Photograph of the Penguin body feather; environmental scanning electron micrographs of (b_1) the rachis and barb; (b_2) the barbules with the hamuli; (b_3) elaborate wrinkles on the barbules and hamuli; (c_1) the tips of barbules without hamuli; and (c_2) oriented nanoscaled grooves on the barbules (~100 nm deep); (d) water contact angle. Reproduced from ref. [49] with permission from American Chemical Society, Copyright 2016.

stainless steel plate, grew ZnO nanohairs on it using crystal growth and obtained post-surface modification by fluoroalkylsilane (FAS). This superhydrophobic micro-nanostructured surface exhibited delayed ice formation (~2 h) at –10 °C. Nguyen et al [60] confirmed that very low top diameter of nanopillars irrespective of height can significantly delay the ice growth. Rajiv et al [61] fabricated thermally- and mechanically-stable superhydrophobic composite coating of multiwalled carbon nanotubes and carbon nanofibers using supercritical fluid method. This composite coating revealed strong repellency towards supercooled water (–20 °C), confirming its anti-icing ability. The composite SiO_2/epoxy resin-based self-cleaning superhydrophobic coating revealed delayed icing as well as low ice adhesion with better stability against bending, twisting, abrasion, strong acid, alkaline, UV light and high temperature resistance (~300 °C) [62–64]. Such superhydrophobic surfaces also inhibit the nucleation [63] and accumulation of ice or snow on the surfaces [64]. Mishchenko et al. [65] reported that at low substrate temperature and high humidity, superhydrophobic surface fully repelled the impacting water droplets well before nucleation.

There are a few disagreements as to whether the superhydrophobic surface having an air-liquid interface could actually show anti-icing performance [66–69]. The disagreements are emanating from the facts of diminishing superhydrophobic property of the surface in high-humidity condition and increasing adhesion character due to large surface area. One particular rough superhydrophobic surface might not be applicable to prevent ice formation at different environmental conditions. The applicability of the superhydrophobic surface for anti-icing mainly depends on the studies carried out with supercooled water (i.e. freezing) and not for in-situ condensed water (i.e. frosting). In extreme cold and humid conditions, water condenses on superhydrophobic surface, get pinned and, hence, fail to exhibit anti-icing ability (Fig. 5a). Cao et al. [66] claimed that all superhydrophobic surfaces may not exhibit anti-icing property. To achieve the anti-icing ability, a precise knowledge on the microstructure (especially in multiple length scales) of the superhydrophobic surface is necessary. Similarly, Chen et al [67] concluded that the superhydrophobic surfaces cannot reduce ice adhesion. In their ice adhesion experiments, both extremely wetting and non-wetting surfaces exhibited similar ice adhesion capability. It is attributed that the ice could get interlocked in the rough structures of superhydrophobic coating, and at the same time, the ice adhesion strength increases linearly with the increase in surface roughness. Also, Varanasi et al [68] observed the buildup of frost on superhydrophobic surface which effectively compromised the anti-icing ability of the surface. Bharathidasan et al [69] reported the low ice adhesion strength on smooth hydrophobic silicone coatings as compared to the rough superhydrophobic coatings. The rough structure of the superhydrophobic coating might get destroyed and detached during ice removal. Bahadur et al [44] developed a model which predicted the ice formation on superhydrophobic surface kept at low temperatures with the impact of supercooled water droplets. By thorough experimental study combined with various phenomena like heat transfer, dynamic wetting, and nucleation theory, it was successfully predicted that the superhydrophobic surfaces can inhibit ice formation. The proposed model can be utilized to fabricate icephobic surfaces by considering the impact of surface microstructure, surface free energy, and thermal properties on ice formation.

Recently, a new class of smart surfaces such as SLIPS have emerged as a possible alternative to superhydrophobic surfaces which have poor mechanical durability due to their high surface roughness. As shown in Fig. 5b, on SLIPS, condensed water drops slide down without pinning due to extremely low contact angle hysteresis. Nguyen et al [70] studied the anti-icing ability of various lubricants that infiltrated porous superhydrophobic aluminum surfaces. The various types of lubricants with different density, viscosity, and surface tension did not have any significant impact on the reduction in ice adhesion. However, a combination of high water repellency of porous surface and infused lubricants effectively reduced the ice adhesion strength on the SLIPS. Zhu et al. [71] fabricated silicon-oil-infused PDMS coatings which efficiently reduced ice adhesion on the surface. Zhang et al [72] prepared a double-layered SLIPS on Mg alloy with coating of double hydroxides-carbonate composite and an infused porous layer on the top consisting of SAMs of 1H,1H,2H,2H-perfluorooctyltriethoxysilane (PTES) with perfluoropolyether (PFPE) lubricant infused in porous layer. This double-layered SLIPS showed excellent corrosion resistance and anti-icing performance. In their review article, Kreder et al. [29] discussed in detail the design of anti-icing surfaces in smooth, textured or slippery form in extreme environmental conditions. Each form of anti-icing

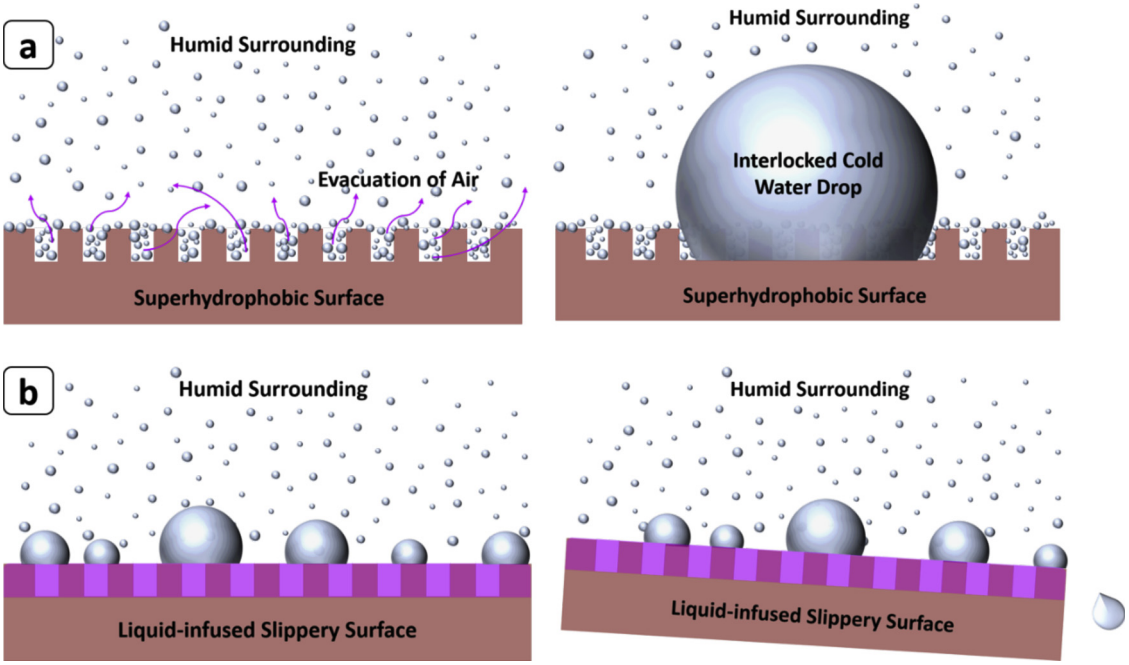

Fig. 5. Schematic illustrating an effect of ice formation in highly cold and humid surrounding on (a) air-infused superhydrophobic surface and (b) liquid-infused slippery surface.

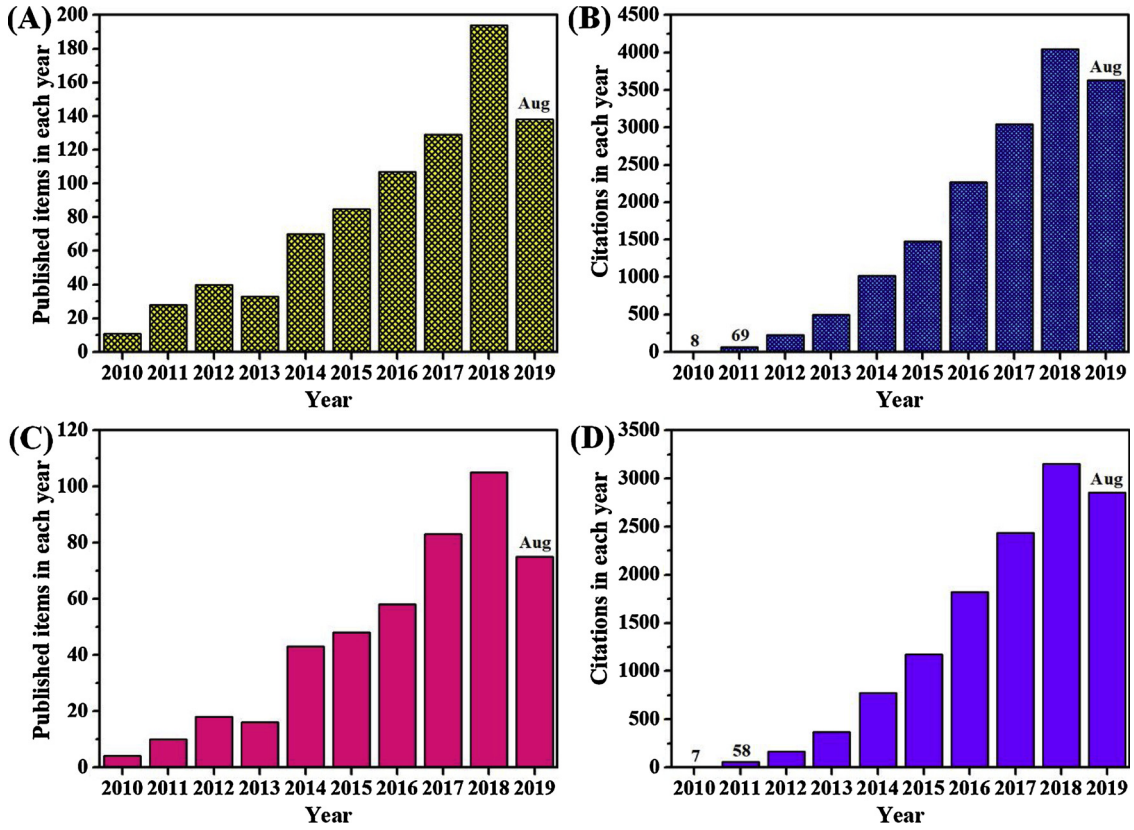

Fig. 6. Numbers of papers published and numbers of times cited from 2010 to 2019 under the topics of (A and B) anti-icing and (C and D) superhydrophobic anti-icing fields (Source: Web of Science).

surface has some limitations during the icing process. Though the rough, textured superhydrophobic surface prevents ice nucleation, it has less humidity tolerance and poor durability during deicing which limit its use in harsh environmental conditions. On the other hand, the smooth anti-icing surfaces can be employed in harsh environments. A systematic research on hydrated surfaces with aqueous lubricating layers are yet to be done. The porous surfaces infiltrated with hydrophobic lubricating layers are promising despite their limited durability during supercooled water drop impact at low temperatures. Fig. 6 illustrates the recent progress in anti-icing as well as superhydrophobic anti-icing fields. The last 10 years of tremendous publications and citations in this arena emphasize the need of materials needed for preventing ice accumulation on substrates to minimize the energy consumption in various types of industries. Herein, we review the different ways of fabrication of superhydrophobic anti-icing surfaces based on polymer coating, nanoparticle/polymer composite coating, and SLIPS, and their advanced applications in anti-icing coatings.

4. Superhydrophobic anti-icing coatings on metals

Metal objects like vehicles, ships, aircrafts, transmission lines, wind turbines and others are subject to accumulation of heavy icing and frosting in low-temperature regions. Recently, considerable attention has been given to the application of anti-icing coating on metal surfaces [73–75]. The surface property of a metal substrate also plays a critical role in the anti-icing behavior [76]. Aluminum is reportedly the best among the various metal substrates used for anti-icing applications due to its versatile applications [73–77]. A metal substrate with smooth morphology can show easy adhesion of water molecules on its surface which eventually becomes ice more rapidly than the metal substrate with hierarchical rough surface morphology [76,77]. Various methods were adopted to develop a hierarchical surface morphology on the aluminum substrate such as anodization, chemical etching, lithography, and salt etching [77,78]. Wang et al [79] adopted wet chemical etching and surface chemical modification method to achieve hydrophobic, sticky, and non-sticky superhydrophobic steel surface. The mixture of hydrogen peroxide and strong acids (i.e., HCl or HNO_3) at different concentrations were used to treat the steel substrates in order to develop micro-nano hierarchical structures and subsequent surface grafting of FAS that rendered the superhydrophobic wettability. A water dripping test (water drop temperature ~0 °C) was performed on the superhydrophobic steel surface treated with hydrogen peroxide/hydrochloric acid at -20 °C. Unlike on bare steel surface, cooled water drops easily rolled off the superhydrophobic steel surface after impact without freezing. In steam-freezing test, no ice film was formed on the superhydrophobic steel surface, confirming its strong anti-icing ability. Moreover, the superhydrophobic steel surface exhibited anti-corrosion ability and preserved its non-wetting ability against tape peeling, sandpaper abrasion, water drop impacting, and UV irradiation. Zheng and researchers [80] employed anodization method (H_2SO_4 electrolyte and anodization voltage of ~20 V for 1 h) with subsequent surface modification by FAS to fabricate hierarchical micro/nanoporous superhydrophobic aluminum (Al) surface. Water drops started to freeze at much lower temperatures (−24 °C) on superhydrophobic-coated Al surface with longer delay (~23 s) in ice formation and low ice adhesion at 0.04 ± 0.02 MPa when compared with pristine Al surface. In addition to superior anti-icing ability, the superhydrophobic aluminum surface exhibited good mechanical durability, stability against corrosive liquids, and self-cleaning behavior.

Apart from superhydrophobic defects, the dust particles existing on the superhydrophobic surface can promote fast icing and frost growth. Hao et al. [81] suggested having dust-free self-cleaning superhydrophobic surface to achieve delay in icing and frost growth with jumping condensates. The surface oxides present on copper foils were removed by HCl treatment and immersed in aqueous solution of 2.5 M sodium hydroxide and 0.1 M ammonium persulfate at temperatures of

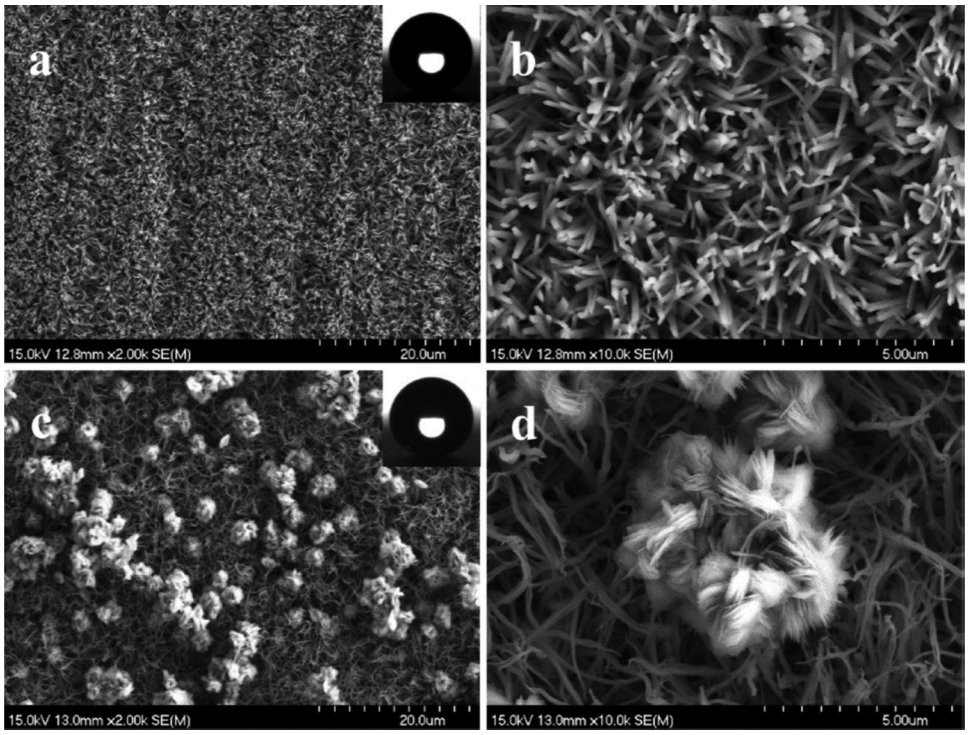

Fig. 7. SEM images of copper surfaces after immersion in aqueous solution of sodium hydroxide and ammonium persulfate for 1 h at (a and b) 4–5 °C and (c and d) 20 °C. Insets showing the shape of water drops with CAs of (a) 159.0 ± 0.7° and (c) 158.2 ± 5.1°. Reproduced from ref. [81] with permission from American Chemical Society, Copyright 2014.

4–5 °C and 20 °C for 1 h followed by dehydration at 180 °C to achieve stable CuO surfaces with uniform nanoribbons and hierarchical nanohair/nanoflower morphology, respectively (Fig. 7). The post surface modification by FAS-17 rendered self-cleaning superhydrophobic property. Two types of condensates, namely, wet or Wenzel type and dry or Cassie type condensates were observed on superhydrophobic CuO surface with hierarchical nanohair/nanoflower and uniform nanoribbons structures, respectively. A delayed Cassie type condensate formed on fine nanostructure of superhydrophobic CuO surface at –10 °C was by the mechanism of jumping freezing and vapor-ice deposition. The impurities in water and surface non-homogeneity also significantly affect the ice adhesion behavior. It is reported that, ice nucleation rate can be relatively lower on a hydrophilic surface than on a hydrophobic surface, owing to surface non-homogeneity of rough hydrophobic surface [82].

Mishchenko and researchers [65] extensively studied the performance of impacting supercooled water drops on flat aluminum (hydrophilic), smooth (hydrophobic) and rough (superhydrophobic) fluorinated Si surfaces which can help to establish the important parameters in proper design of anti-icing surfaces. The ice accumulation ability experiments were performed on tilted hydrophilic, hydrophobic and superhydrophobic surface kept at –10 °C by impinging a stream of cooled water droplets from a height of 10 cm as shown in Fig. 8A. A delayed ice formation (~1 min) on hydrophobic surface as compared to hydrophilic surface was noticed. However, substantial ice accumulation on both the surfaces was observed at about 10 min. Mere chemical modification of a smooth surface did not delay the ice formation and accumulation as compared to a pristine smooth surface. However, on rough superhydrophobic surface (microstructures like posts, bricks, blades, and honeycombs achieved on Si surface by Bosch process), no signs of ice accumulation were observed even after 10 min. A single water drop impact test was also performed by capturing images of droplets' impact, maximum spreading, maximum retraction, and freezing on the same three surfaces arranged in tilt (30°) and horizontal positions Fig. 8(B and C). At both these positions, the behavior of water drops on the substrates was the same. No retraction of water drops on hydrophilic surfaces was detected, confirming instant freezing on the substrate ($T_{substrate} < -10$ °C). On smooth hydrophobic surface, a significant retraction of water drop was noticed. However, it remained pinned and frozen on the surface ($T_{substrate} < 0$ °C). In comparison, water drops bounced off with complete retraction and without freezing on superhydrophobic surface kept at $T_{substrate} > -25$ to –30 °C. The superhydrophobic surfaces with uniform microstructure effectively avoided ice nucleation and subsequent freezing.

Wang et al. [83] applied thin fluorocarbon coating of less than 10 nm on copper substrate to achieve superhydrophobicity. A comparative icing process on plain and superhydrophobic copper surface was studied as shown in Fig. 9A. A water drop on plain copper surface achieved CA ~84° with hemispherical shape possessing a large contact area, and icing starts at 180 s. However, icing was initiated at around 220 s on superhydrophobic copper surface due to reduced contact area of ball-shaped water drops. The time taken for complete icing on superhydrophobic copper surface was much higher than on plain copper surface, confirming the delayed icing formation. Boinovich et al [64] studied the robustness and anti-icing behavior of superhydrophobic stainless steel surface by subjecting it to outdoor snow and ice accumulation. The stainless-steel substrates were etched in aqueous ferric chloride for multiple times, and the obtained rough substrates were coated by a suspension of silica nanoparticles and fluorooxysilane to achieve superhydrophobicity. The fabricated superhydrophobic stainless steel surface exhibited WCA of 155° and roll off at 42° after 100 repeated icing/deicing cycles. For comparison, the pristine and superhydrophobic stainless steel sheets were exposed to outdoor heavy snowfall at −3 °C, 99% humidity and wind velocity of 2 m/s (Fig. 9B). The falling wet snow remained stacked on pristine steel surface followed by accumulation, whereas low adhesion of snow was found on superhydrophobic steel that can easily get removed under wind flow or mechanical vibration. The delayed freezing was observed on the superhydrophobic steel when subjected to freezing rain (−6 °C).

Wang et al [84] achieved flower-like hierarchical structure on stainless steel through wet chemical etching using sulfuric acid and hydrogen peroxide, and the surface energy was lowered by grafting silanes, particularly on FAS on the surface. The prepared superhydrophobic steel surface exhibited anti-icing ability in condensing test, where the temperature of the assembly was dropped from 40 °C to-20 °C. The time for freezing was lowered due to the development of

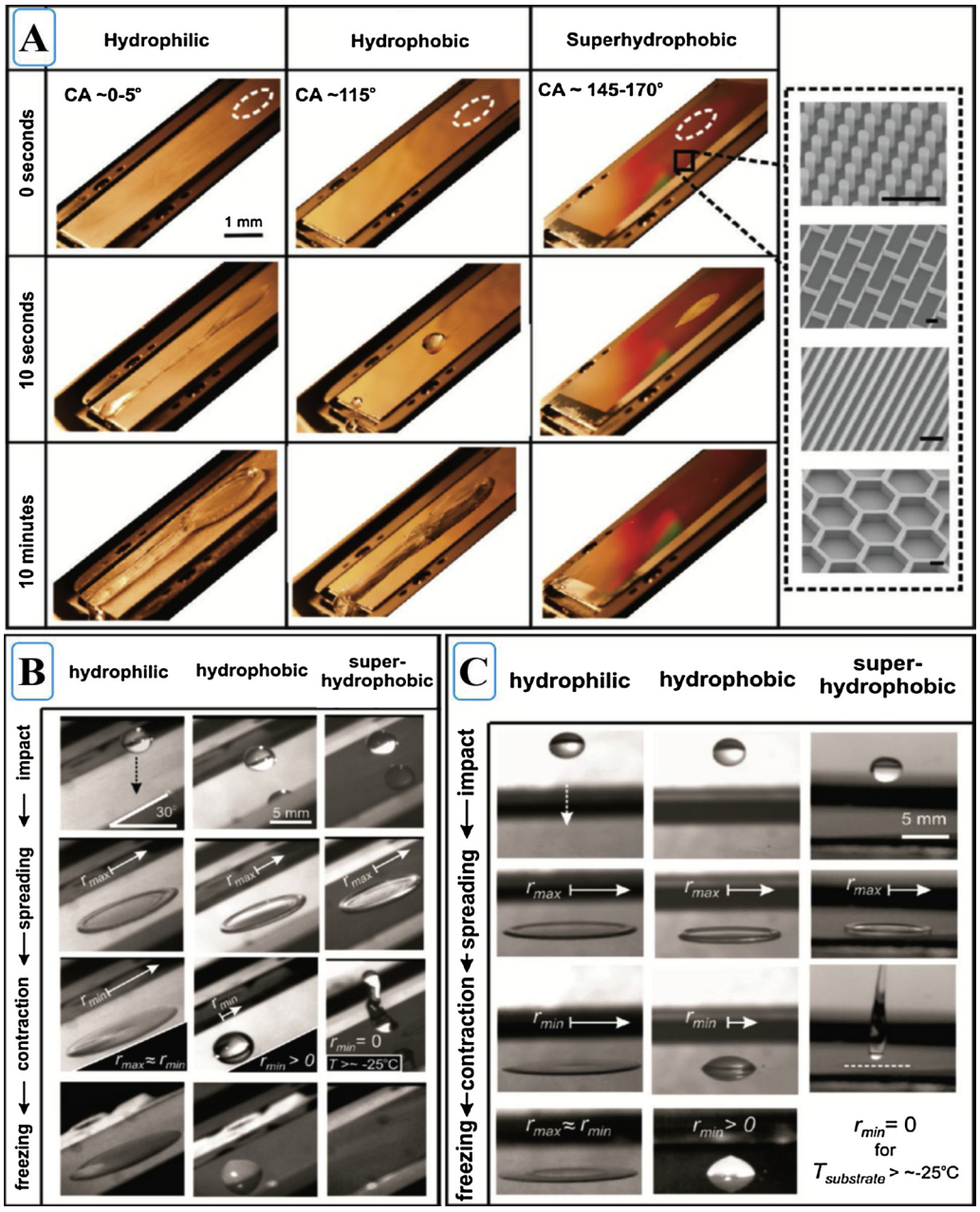

Fig. 8. (A) Ice formation and accumulation on flat aluminum (hydrophilic), smooth fluorinated Si (hydrophobic) and rough fluorinated Si (superhydrophobic) surfaces at different time frames. Insets depicts various microstructures like posts, bricks, blades and honeycombs (scale bars: 10 μm) of superhydrophobic surfaces. Series of images of the dynamic behavior of ~ 15 μl single droplets impinging on (B) 30° tilted and (C) horizontal surfaces ($T_{substrate}$ < 0 °C) from a height of 10 cm. Top to bottom images reveals droplet impact, spreading, retraction and freezing. Reproduced from ref. [65] with permission from American Chemical Society, Copyright 2010.

small spherical condensed water drops on the surface. The superhydrophobic wettability of the surface was sustained even after 20 icing/de-icing cycles. To avoid the post surface chemical modification, Cheng et al [85] adopted a two-step immersion etching process and subsequent heat treatment to fabricate highly superhydrophobic aluminum surface for anti-icing and anti-corrosion application. The aluminum substrates were first immersed in sodium hydroxide solution and subsequently immersed in aqueous copper chloride solution to achieve hierarchical surface structure which exhibited superhydrophilic wettability. The wettability of the surface was switched to superhydrophobic state via thermal treatment (150 °C for 2 h) due to the formation of oxides and nano-sized particles on dendritic structure. During icing experiments (–15 °C in refrigerator), icing starts on untreated aluminum surface after 20 min and freezes completely at around 40 min, whereas the icing starts on superhydrophobic aluminum surface after 40 min, confirming its delayed ice forming ability.

5. Polymer based anti-icing coatings

The applicability of robust anti-icing coating on different substrates of various shapes and sizes is the most desirable. Polymers are promising candidates that can achieve durable coating due to their excellent toughness character. Yuan et al [86] have studied the anti-icing characteristics of highly superhydrophobic coating prepared from low-density polyethylene (LDPE). The LDPE coating resembled the surface morphology of the lotus leaf with the surface wettability of CA ~156 ± 1.7° and the low sliding angle of ~1°. The sticky and non-sticky types of superhydrophobic LDPE-coated materials were kept at –5 °C and supercooled water droplets (diameter ~1 mm) were sprayed from the height of 20 cm. In the non-sticky LDFE surface, the sprayed water droplets rolled off very quickly for 60 min of continuous spraying without icing, whereas the ice was completely covered on sticky LDFE surface after 7 min of spraying. Hong et al [87] adopted a simple, one-step precipitation polymerization method to develop mechanically durable anti-icing superhydrophobic coatings. Yang et al [88]

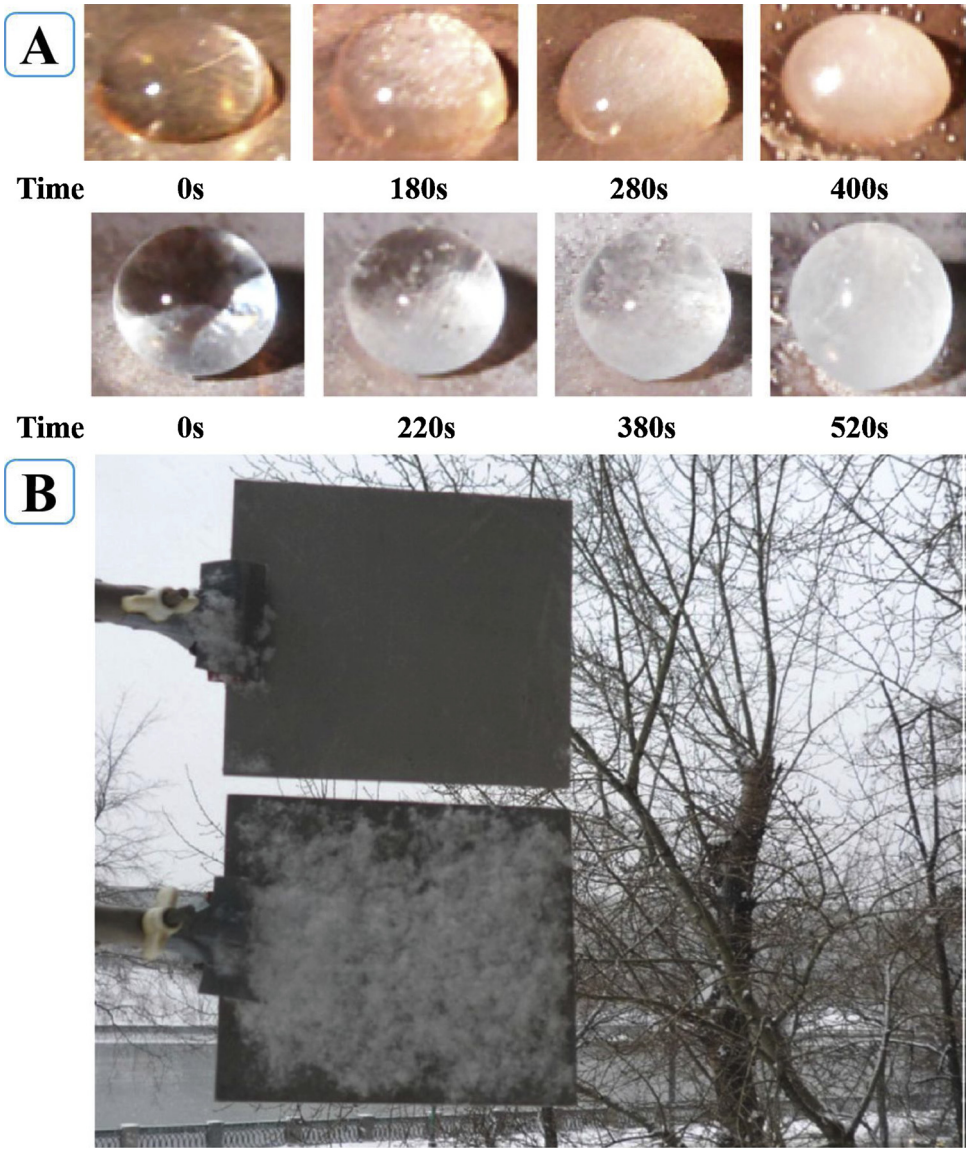

Fig. 9. (A) An icing process of water droplet on plain copper surface (top) and superhydrophobic copper surface (bottom), Reproduced from ref. [83] with permission from Elsevier, Copyright 2012. (B) An exposure of superhydrophobic stainless steel (top) and pristine stainless steel (bottom) to outdoor heavy snowfall. Reproduced from ref [64]. with permission from American Chemical Society, Copyright 2013.

developed a physical model explaining air cushion convection in porous self-cleaning superhydrophobic polymer (PTFE/PPS) coating (WCA ~ 162° and WSA ~ 3°) based on their experimental results, which efficiently delayed the icing process. Polyphenylene sulfide (PPS) resin mixed with water-soluble PTFE emulsion was spray-coated on different metals such as stainless steel, aluminum, and copper substrates. Then the hierarchical and uniform porous network in the coating was achieved by decomposing ammonium carbonate and nonionic surfactant (Fig. 10A). During anti-icing experiments, water drops were placed on polymer coating in an environment of warm turbulent airflow. Formation of air-film during heat and mass exchange phenomena delayed the icing of water drops. The ice nucleation on the surface started as soon as the air cushion convection vanished. As shown in Fig. 10B, the air cushion effect and icing behavior of water droplet on bare and self-cleaning superhydrophobic steel were tested in a refrigerator at –20 °C. The shapes of water drops on both the surfaces remain unchanged after 10 min freezing and 2 min melting (Fig. 10B, a-c and e-g). The point of contact area of ice beads was noticeable and were lifted by the stable air cushion in the superhydrophobic coating. After bringing the surfaces to ambient temperature, spherical water drops quickly rolled off the porous superhydrophobic polymer coated steel.

Most of the reported anti-icing polymer used are not particularly superhydrophobic but hydrophobic or hydrophilic in nature with low roughness. Dou et al [57] reported the durable anti-icing polyurethane (PU)-based polymer coating on metal, alloys, plastic, and ceramic substrates by spin coating. A PU dispersion was prepared by covalently attaching the hydrophilic components on the polymer chain. This dispersion was added to a mixture of water and isophorone diamine (IPDA) for chain extension. As PU chains possessed both the hydrophilic and hydrophobic groups, spherical particles were formed with hydrophobic core and hydrophilic corona with ultra-rough coating and hydrophilic wettability of CA ~43°. The ice adhesion strength on the hydrophilic PU coating was significantly reduced to 27.0 ± 6.2 kPa when compared with the uncoated substrate (800 kPa), due to the presence of aqueous lubricating layer between ice and coating. The formation of aqueous lubricating layer can be reasoned to the absorption of water by the hydrophilic corona during icing process, leading to the melting of ice. The ice adhesion was low even after the temperature was lowered to −53 °C. The accumulated ice on the coating was simply blown off with the aid of wind having the velocity of 12 m/s (Fig. 11A),

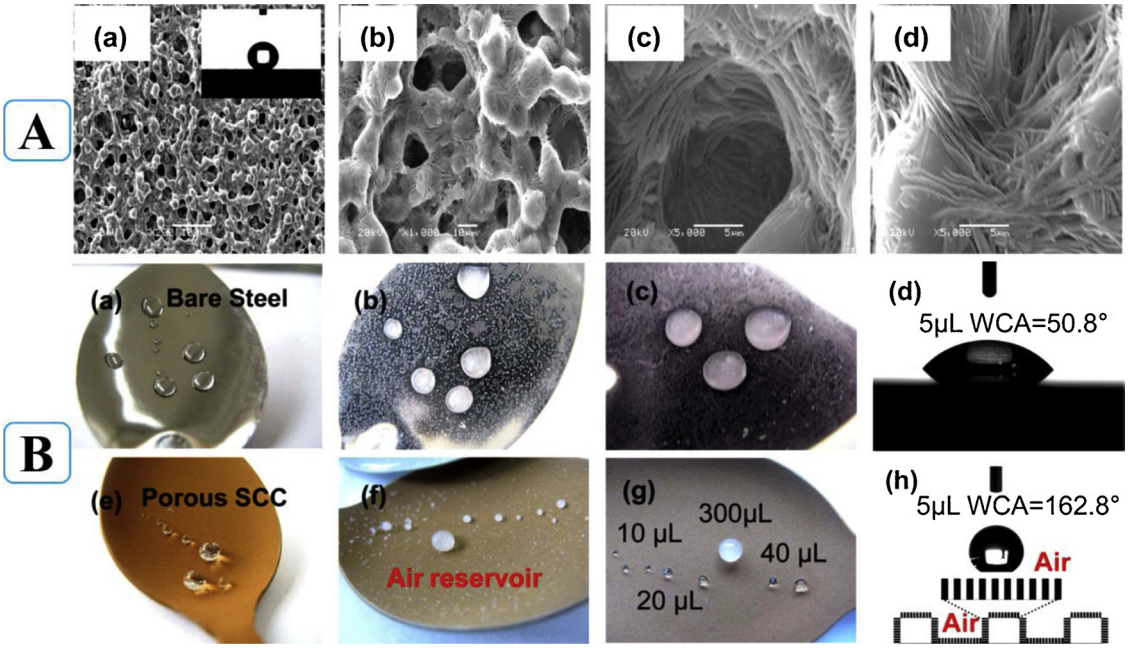

Fig. 10. (A) SEM micrographs of porous self-cleaning superhydrophobic PTFE/PPS coating at different magnifications (a–d). (B) Optical photographs of water droplet on curved bare steel (top) and curved self-cleaning superhydrophobic coating (bottom) (a, e) in the atmosphere, (b, f) at −20 °C after freezing for 10 min, (c, g) after melting for 2 min, (d, h) WCAs measured using 5 μL water drops. Reproduced from ref. [88] with permission from American Chemical Society, Copyright 2016.

whereas the ice stayed firmly on the uncoated surface even at the wind velocity of ~30 m/s. PU coating maintained the ice adhesion strength of ~27.0 kPa even after 30 repeated icing/de-icing cycles. In addition, the anti-icing PU coating applied on copper, steel, aluminum, ceramic, aluminum alloy and rubber exhibited a significant reduction in ice adhesion strength (~30.0 kPa) (Fig. 11B). Li et al [89] developed an optically transparent anti-fogging and anti-icing coating by casting polyhedral oligomeric silsesquioxane-poly[2-(dimethylamino)-ethyl methacrylate]-block-poly(sulfobetaine methacrylate) (POSS-PDMAEMA-b-PSBMA) with ethylene glycol dimethacrylate (EGDMA) on glass substrate followed by UV-curing. The self-lubricating aqueous layer appeared on amphiphilic POSS-PDMAEMA-b-PSBMA coating and effectively delayed freezing at –15 °C for 120 s. Koivuluoto et al [90] adopted flame spraying method to fabricate PE-based hydrophobic polymer coatings on metals and studied their anti-icing performance. It was noted that the increase in ice adhesion increased the surface roughness of the coating. The ice adhesion strength of ~54 kPa observed in PE coating at –10 °C was seven times lower when compared with bare substrates under the same conditions. Ng et al [91] prepared durable icephobic coating on PU topcoat by a simple casting method using copolymers such as poly(methyl methacrylate) and poly(lauryl methacrylate-2-hydroxy-3-(1-amino dodecyl)propyl methacrylate) with a small addition of paraffin wax, which induces hydrophobic microdomains on wrinkled patterns. This heterogeneous microstructure facilitated delayed icing on the surface and inhibited icing propagation after nucleation. Compared to plain PU topcoat, the paraffin-modified PU topcoat exhibited reduced ice adhesion strength (about 47%) and 70% energy savings in de-icing. He et al [92] analyzed 22 polymer-based hydrophilic and hydrophobic surfaces at room temperature and compared their ice adhesion strength capabilities. This research established that the WCA, surface roughness and toughness of the polymeric surfaces did not affect their ice adhesion strength, and instead, their low elastic modulus led to low ice adhesion.

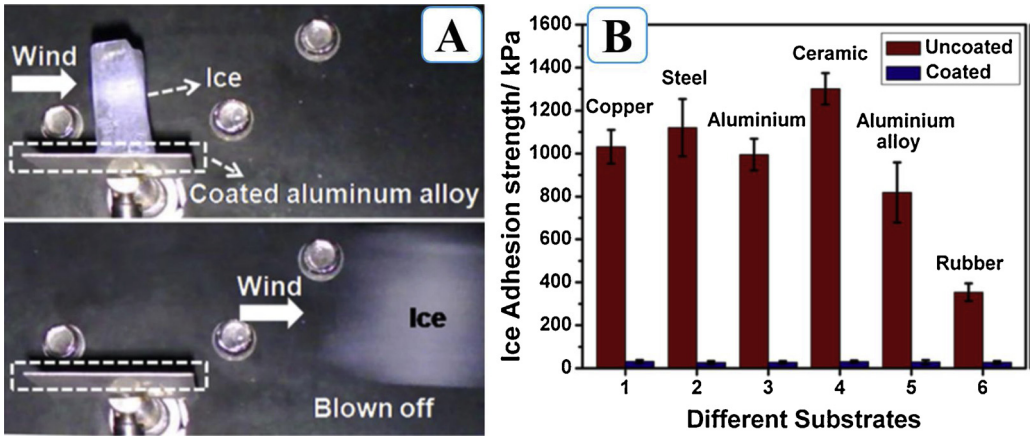

Fig. 11. (A) The adhered ice on the anti-icing PU coating was blown off with the action of wind. (B) Ice adhesion strength on various substrates before and after anti-icing coating. Reproduced from ref. [57] with permission from American Chemical Society, Copyright 2014.

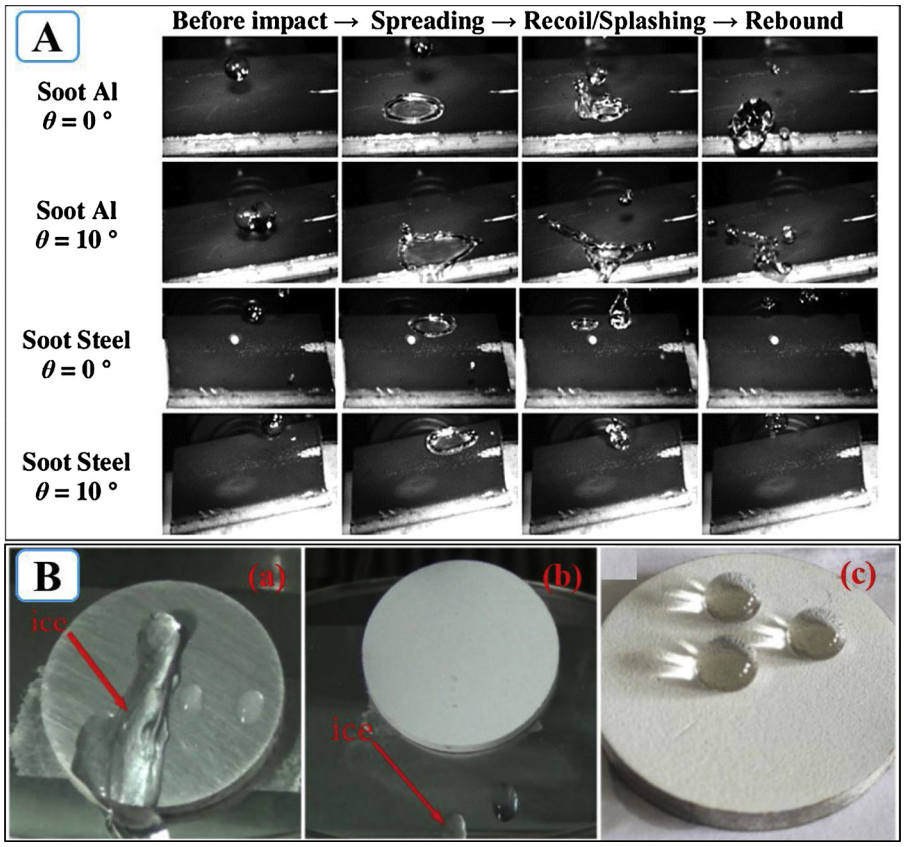

Fig. 12. (A) Supercooled water drop impact study on the superhydrophobic carbon soot coated aluminum and steel surfaces kept in horizontal (θ = 0°) and tilted positions (θ = 10°). (Water drop impact height ~ 7 cm, $T_{substrate}$ = – 30 °C, Relative humidity ~ 100%, Frame time = 500μs). Reproduced from ref. [93] with permission from Elsevier, Copyright 2016. (B) Supercooled water dripping on (a) bare steel substrate and (b) superhydrophobic coating, (c) Water droplets on the superhydrophobic coating after dripping test. Reproduced from ref [95]. with permission from Elsevier, Copyright 2016.

6. Nanoparticle/polymer composite based superhydrophobic anti-icing coatings

Utilization of carbon materials for anti-icing coating is a developing area of research. Esmeryan et al. [93] utilized cheap candle soot particles and facile deposition strategy to develop anti-icing coating on aluminum and steel. The pre-cleaned substrates were held on chimney flame with rapeseed oil for 20 s, dipped in ethanol and then immersed in emulsion of block copolymer consisting of perfluorocarbon and polyvinylalcohol. The addition of perfluorocarbon ensured better adhesion of the candle soot to the substrate and improved the mechanical durability of the coating. The superhydrophobic wettability of the coating was established under repetitive icing/de-icing cycles, spinning, water jetting, and harsh air scavenging. At ~–35 °C, the horizontal and tilted superhydrophobic aluminum and steel surfaces exhibited icephobic property against the impact of supercooled water droplets (Fig. 12A). Under the action of capillary forces after impact and spreading on the superhydrophobic carbon soot coating, water droplets eventually rolled off the surface, well before nucleation. In addition, the water droplets retained its spherical shape upon freezing and easily got detached after receiving a mild thermal energy, confirming the reduced ice adhesion observed on the coating. However, on bare aluminum and steel substrates, the supercooled water drops exhibited negligible retraction, confirming immediate freezing on the surface. Zhang et al [94] determined that surface chemistry and intrinsic contact angle played an important role in anti-icing performance of the surface. Authors have tuned the roughness of the carbon nanotube (CNT) surfaces by chemical vapor deposition (CVD) and separately deposited thin layers of 1H,1H,2H-perfluoro-1-dodecene (PF), hexamethyldisiloxane (HMDSO), and maleic anhydride (MA) by plasma-enhanced chemical vapor deposition (PECVD) to achieve three different surface chemistries on CNTs. Among all, PF-coated CNT surface exhibited higher intrinsic contact angle (θ ~106°) when compared with MA surface (θ ~44°). The PF-coated CNT surface exhibited superhydrophobic property (at −2 °C) with stable Cassie-Baxter state for water drops and had excellent anti-icing performance and lower amount of frost formation as compared to HMDSO/CNT, MA/CNT and CNT surfaces.

The use of silica nanoparticles in the fabrication of nanoparticle/polymer composite superhydrophobic coating for anti-icing application is well known. Pan et al. [95] spray-coated the hydrophobic silica nanoparticle/PMMA suspension on steel surface to achieve superhydrophobic coating with WCA ~ 158° and SA ~ 2° and tested its anti-icing behavior by supercooled water dripping and in condensed environment (–20 °C). During supercooled water dripping test (Fig. 12B), the supercooled water drops rolled off the superhydrophobic coating without any trace of icing on the surface; this is in contrast to the behavior on bare steel surface where the ice formation was observed under the same conditions. The superhydrophobicity of the coating was retained after the dripping test [Fig. 12B(c)]. Liu et al. [96] have spin-coated a dispersion of silica nanoparticles in polystyrene/chloroform on glass and aluminum substrates and subsequently calcinated at 550 °C (to remove organic elements) to obtain a coating with fused silica nanoparticles. Then, a thin self-assembled monolayers (SAM) of 1H,1H,2H,2H-perfluorooctyltriethoxysilane (POTS) were obtained on silica coating by CVD to achieve superhydrophobicity. The POTS-coated materials exhibited lower ice adhesion strength (< 100 kPa), were durable and highly porous microstructure, enabled the trapping of tiny air pockets, and efficiently delayed the icing (~289 s), as compared to bare substrate (~24 s) and commercial icephobic surfaces (~204 s). Zhan et al. [97] synthesized hybrid silica nanoparticles with anti-icing superhydrophobic surface with hierarchical roughness by effectively grafting the fluorinated polymer chains to silica nanoparticles. This was achieved by surface-initiated activators generated by electron transfer atom transfer radical polymerization followed by spin coating on glass substrate. At −18 °C, a delay of nearly 168 min was observed for the water drop to freeze on this superhydrophobic coating. Shang and co-researchers [98] studied self-cleaning and anti-fogging properties of a highly transparent and porous superhydrophobic silica

coating prepared on glass substrate through layer-by-layer assembly of raspberry-like polystyrene@silica microparticles followed by calcination. This porous superhydrophobic silica coating showed excellent anti-icing ability and anti-fogging property. Caldona et al [99] achieved a superhydrophobic surface with excellent anti-icing, anti-corrosion and oil-water separation capability by using a mixture of infused silica nanoparticles in the rubber-modified polybenzoxazine. Wu and Chen [100] prepared an optically transparent and mechanically durable sol-gel processed superhydrophobic silica coatings which significantly opposed the condensation of water droplets. Also, numerous efforts have been made to fabricate green waterborne, self-healing superhydrophobic silica coatings for outdoor anti-icing [101].

Nanoparticles of metal oxides such as Al_2O_3, ZnO, and CeO_2 have also been utilized to fabricate composite nanoparticle/polymer anti-icing coatings. Momen et al. [102] compared the anti-icing behavior of superhydrophobic surfaces of Al_2O_3 prepared by spin as well as spray coat techniques. A suspension of 14 wt% alumina nanoparticles in silicone rubber/hexane was coated on aluminum substrates by both methods. The spray-coated sample (non-uniform flower-like microstructure) was rougher than spin-coated sample (uniform spongy-like morphology) and had similar WCA and CAH. A spin-coated sample exhibited low ice adhesion strength (~65 kPa) when compared to bare aluminum (~316 kPa). However, after 12 icing/de-icing cycles in spin-coated samples, an increase in ice adhesion strength as well as decrease in superhydrophobicity was observed. This was reasoned to the supercooled water drop penetrating inside the rough structure with increased contact area that damaged the rough coating surface during de-icing. However, in case of rougher spray-coated sample, ice adhered firmly to the surface, confirming its negligible anti-icing ability. This study established that rougher and irregular surface morphology of superhydrophobic coatings lead to poor anti-icing behavior. Wang et al [103] developed a flexible and lightweight icephobic novel substrate by creating micro/nanostructure on glued tape. In a typical fabrication of icephobic glued tape, the poly(vinylidene fluoride) (PVDF) microspheres were pressed on glued tape, and three different nanostructures of ZnO, namely, nanoparticles (NPs), nano-cones (NCs), and nano-hexagonal rods (NHRs) were decorated on PVDF microspheres by crystal growth method. At -10 °C, the resulting surfaces exhibited WCAs of nearly 122°, 162° and 160° at 10 °C and icing delay times of approximately 7 min, 126 min, and 118 min, respectively. The ice adhesion force on NCs and NHRs were less than 55 μN and 72 μN at -10 °C. Water drops were pinned on NPs at −2 °C and were easily removed from the NC surface. However, when kept at -15 °C for 2 h, the ice drops remained pinned on the NP surfaces. NC and NHR surfaces revealed better icephobic properties than NPs due to the existence of pocketed air between the liquid and solid. Yang et al. [104] coated a suspension of 30 wt% 1-dodecanethiol (DT)-modified ZnO particles in PDMS on aluminum substrates by drop coating followed by sandpaper abrading method. The effect of both temperature (-5° to -15°) and tilting angle (~0° to 10°) on anti-icing behavior of the prepared superhydrophobic ZnO/PDMS composite coating was analyzed. A delayed ice formation and reduced ice adhesion strength was observed at lower temperatures and tilting angle as compared with bare aluminum substrate. A stable wettability of the surface was also observed after 10 icing/de-icing cycles. By simple and quick sandpaper abrasion strategy, the damaged ZnO/PDMS composite surface observed after multiple cycles was repaired, and the superhydrophobic wettability was restored.

Fu et al [105] demonstrated a very facile, straightforward and low-cost preparation of anti-icing superhydrophobic cerium dioxide/polyurethane nanocomposite coatings by hydrothermal method. The cerium dioxide nanocomposite coatings with superhydrophilic (without stearic acid coating), hydrophobic (with polyurethane on smooth and etched aluminum alloy substrates) and superhydrophobic (with stearic acid coating) wetting properties were analyzed for their anti-icing behavior at different temperatures under static and dynamic circumstances. The water drops were completely retracted and rebounded off the superhydrophobic coating at low temperatures irrespective of impact velocity. It was observed that the stearic acid-coated samples maintained the superhydrophobicity even at freezing temperatures and also exhibited icephobic behavior after numerous icing/de-icing cycles. Tong et al [106] also adopted chemical etching of aluminum surface and post surface modification by stearic acid to achieve superhydrophobic anti-icing capability. Nagappan et al. [107] developed a thermally stable non-stick superhydrophobic surface on a glass substrate by using polymethylhydrosiloxane and multi-walled carbon nanotube hybrid materials. The hybrid material exhibited an excellent anti-icing performance with prevention of icing for 48 h and showed the liquid as marble-like non-stick water droplets. Hashmi et al. [108] and Zang et al. [109] also studied the freezing of liquid-marbles on the superhydrophobic surfaces. Their experiments suggested that the large size of liquid marbles can delay icing on the superhydrophobic surface when compared with the smaller analogs.

7. Slippery liquid-infused porous surfaces (SLIPS) based anti-icing coatings

In nature, two types of anti-wetting surfaces exist, namely, lotus leaf surface as a superhydrophobic and pitcher plant surface as a lubricant-infused “slippery” surface. The ice-phobic surfaces are generally obtained by using the principle of lotus-leaf inspired superhydrophobic surfaces. However, these surfaces have a drawback of water condensation, frost formation, and increased ice adhesion due to a large surface area at high humidity conditions. Recently, to circumvent the challenges associated with superhydrophobic surfaces, the characteristic features of pitcher plant surface elucidated by Bohn and Federle [50] were utilized to build anti-icing SLIPS. Inspired from multifunctional pitcher plant, Wong and researchers [54] pioneered SLIPS for the first time consisting of a micro/nanoporous surface infiltrated by an immiscible lubricating liquid forming a smooth and homogeneous film (Fig. 13a). Two different types of porous surfaces were fabricated, namely, ordered epoxy-resin based arrays of nanoposts modified by FAS and random Teflon-based porous nanofibre surfaces (Fig. 13b). The low-surface tension perfluorinated liquids (lubricant) infiltrated into the porous substrates, forming a homogeneous and smooth surface of roughness nearly 1 nm. The fabricated SLIPS exhibited extremely low contact angle hysteresis less than 2.5° and, hence, repelled a range of liquids such as light crude oil, blood, (Fig. 13c, d) water, and hydrocarbons. At −4 °C and relative humidity of 45%, the SLIPS had no ice adhesion (Fig. 13e) and took only milliseconds to repair the physical damage and sustain the wettability as before. The lubricant infused inside the porous structures was undisturbed even at high applied pressure of about 680 atm. Fig. 13f demonstrates the failed attempts of the carpenter ant to hold on to SLIPS and eventually slipped after tilting (mimic of pitcher plant surface). On the other hand, the ant firmly held onto a normal flat teflon based hydrophobic substrate. Kim et al. [52] have fabricated SLIPS-coated aluminum surface which efficiently reduced ice/frost accumulation as well as ice adhesion strength. In this method, polypyrrole (PPy) was coated on aluminum substrates by electrodeposition followed by hydrophobic modification using chemical vapor deposition of (tridecafluoro-1,1,2,2-tetrahydrooctyl)trichlorosilane. Subsequently, SLIPS was prepared by adding a few drops of perfluoroalkylether lubricant on hydrophobic PPy-coated aluminum substrates having lubricant layer thickness of nearly 8-10 μm. The condensed water drops rolled off quickly before freezing on SLIPS-coated aluminum surface, and the accumulated ice was removed off under gravity at low tilting angle. These materials possessed a very low ice adhesion strength of ~15 kPa and were useful in outdoor anti-icing applications.

Wang and researchers [110] prepared a stable porous superhydrophobic surface by pouring hot uniform suspension of hydrophobic silica nanoparticles, ultra-high molecular weight polyethylene and decahydronaphthalene on various substrates (Steel, Al, Cu, Ti and PET

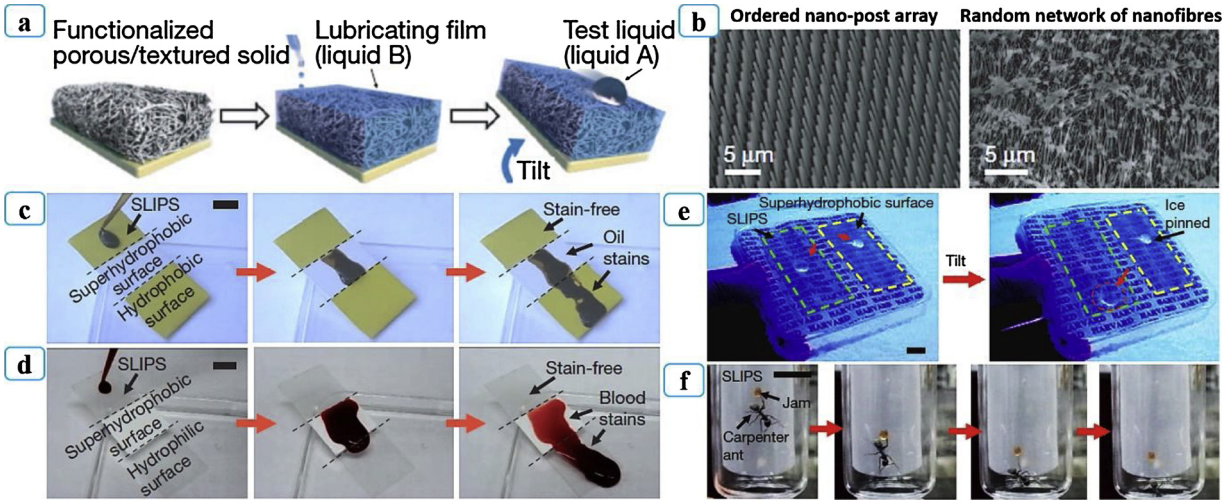

Fig. 13. (a) Schematic depicting the fabrication of SLIPS by infusing lubricating liquid in porous solid, (b) SEM images of ordered epoxy-resin based arrays of nanoposts modified by FAS (left) and random Teflon-based porous nanofibre surface (right), (c) Dynamic behavior of light crude oil on a surface composed of a SLIPS, a superhydrophobic Teflon porous membrane and a flat hydrophobic surface, (d) Anti-wetting ability of SLIPS, a superhydrophobic Teflon porous membrane and a flat hydrophilic glass substrate towards blood, (e) Ice adhesion behavior on SLIPS (highlighted in green) and ordered epoxy-resin based superhydrophobic surface (highlighted in yellow) during outdoor exposure with temperature of −4 °C and relative humidity of 45%. (f) Demonstration of the failure of a carpenter ant to hold on to SLIPS and eventually slide with fruit jam along the SLIPS upon tilting. Scale Bars ~ 1 cm. Reproduced from ref. [54] with permission from Springer Nature, Copyright 2011.

substrates) which exhibited excellent mechanical durability against abrasion, corrosion, tape peeling and drop impact. However, at low temperatures (< 0 °C), water drops got pinned on the prepared superhydrophobic surface, exhibiting poor anti-icing ability. Hence, SLIPS were prepared by infusing different lubricant liquids (perfluorotripentylamine, kerosene and silicon oil) in the superhydrophobic surface. At -20 °C, water drop smoothly slided off the SLIPS, whereas the water drop remained pinned on superhydrophobic surface at all temperatures. The same research group [111] fabricated highly porous superhydrophobic coating by spray-coating suspension PMMA/fluorinated SiO_2 on the substrates, which exhibited extremely water repellent and oleophilic properties. A subsequent infusion of perfluorotripentylamine (Fluorinert FC-70) lubricant in the porous structure of superhydrophobic coating resulted in lyophobic SLIPS, which exhibited repellency towards a range of low surface tension liquids such as water, kerosene, hexane, diesel oil, and milk. Different parameters controlling the travelling speed of the various liquids on SLIPS were also detailed by the same authors. Various liquids with comparable weights such as hexane (m = 0.032 g), kerosene (m = 0.041 g), diesel oil (m = 0.042 g), water (m = 0.050 g) and milk (m = 0.051 g) exhibited different travelling speeds (Fig. 14a–e). The travelling speeds of 1.15, 0.63, 0.55, 0.65, and 0.30 cm/s were recorded for hexane, kerosene, diesel oil, water and milk drops on SLIPS, respectively. It was noted that the travelling speed of liquid drops on SLIPS was not dependent on the weights but on their kinematic viscosities (Fig. 14f). On the SLIPS kept at –20 °C, the water drops moved freely without pinning due to the negligible formation of capillary bridge, exhibiting efficient anti-icing performance. Liu et al [112] have fabricated optically transparent omniphobic coatings by infusing fluorinated lubricant in a spin-coated PTFE nanoparticulate film, which showed excellent anti-icing property. Cao et al. [113] have thoroughly studied and compared the wetting properties, anti-fogging, self-cleaning ability, droplet impact, and optical transparency of lotus leaf-based superhydrophobic and pitcher plant-based lubricant infiltrated slippery surfaces. The silicone-based superhydrophobic (SUB) coating (WCA ~ 150° ± 2°, SA ~ 4.3° ± 0.4°, optical transparency < 10%) on glass substrate was prepared from the homogeneous suspension of hydrophobic fumed silica nanoparticle/poly(dimethylsiloxane) through dip coating. The liquid-infused slippery (LIS) surface (WCA ~ 96° ± 1°, SA ~ 7.8° ± 1.2°, optical transparency ~ 90%) was obtained by simple absorption of silicone oil on SUB surface. Both the SUB and LIS surfaces have advantages as well as disadvantages. However, depending on the need at different environmental conditions, suitable surface can be effectively selected. Recently, Zhang et al [114] used cheap lubricant liquids such as polyols to infiltrate the inside porous structure consisting of magnetic nanoparticles, which exhibited thermal de-icing capability.

8. Outdoor applications of superhydrophobic anti-icing coating

Continuous efforts have been made and are still in progress to scale-up anti-icing coating for industrial applications. Parent *el. al* [41] have briefly described various anti-icing and de-icing techniques used for wind turbines and discussed their advantages as well as disadvantages. Three decades before, the de-icing of wind turbines was done by direct warming of blades. However, in recent times, development of anti-icing superhydrophobic or SLIPS led to efficient inhibition of ice adhesion. Peng and co-researchers [115] used dispersion of PVDF/ammonium bicarbonate powder for coating a wind turbine blade. A highly porous superhydrophobic coating was obtained with very low sliding angle (~2°) of water drop. To simulate natural icing environment, the coated turbine blades were held in a chamber at –10 °C for 30 min, and supercooled water drops (diameter ~1 mm) were sprinkled from the height of 20 cm. The supercooled water drops rolled off the superhydrophobic wind turbine, and no trace of ice formation was observed even after 60 min of constant spraying, proving the strong anti-icing ability of the coated material. Li et al. [116] have applied superhydrophobic coating on glass insulators by spray-coating the suspension of PDMS/hydrophobic silica nanoparticles. The anti-icing ability of the prepared superhydrophobic coatings (WCA ~161°) were compared with room temperature vulcanized (RTV) silicone rubber hydrophobic coatings (WCA ~110°). During water flow test at room temperature, water bounced off the superhydrophobic coating, whereas hydrophobic coating formed a flowing thin water film. This was attributed to the lower contact area in superhydrophobic coating when compared with hydrophobic coating. Further, both the superhydrophobic and hydrophobic coatings were kept at –5 °C and sprayed with water drops of diameters nearly 80 µm through fog nozzles (Fig. 15a and b). After 10 min, ice formation was noticed on hydrophobic coating, whereas no

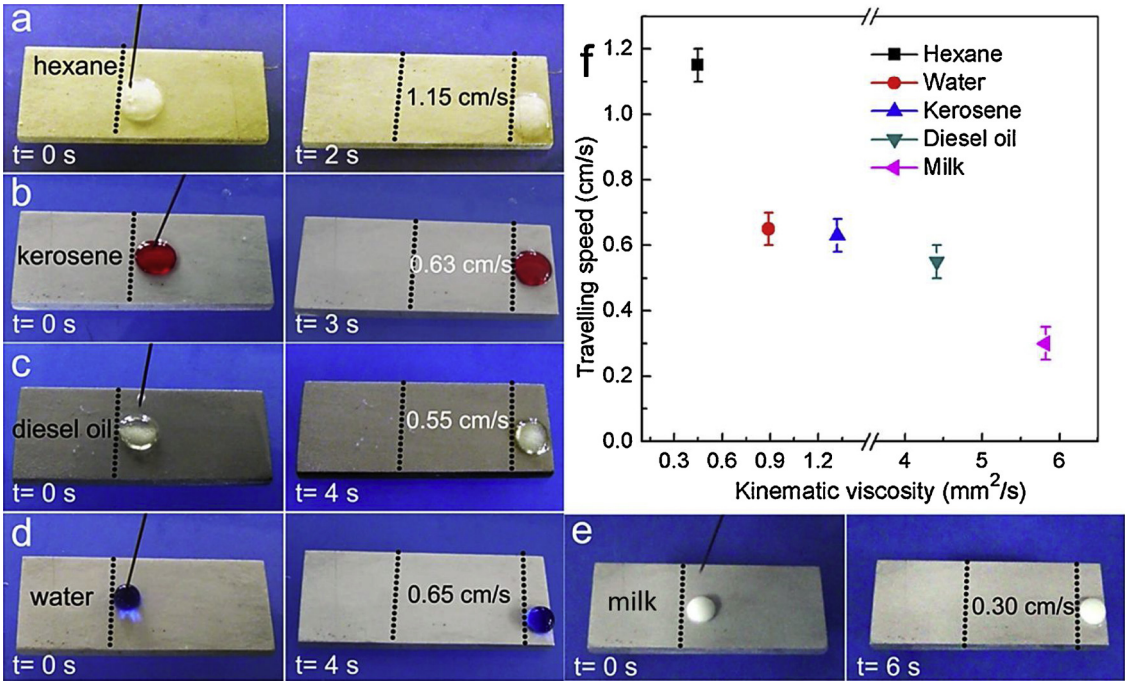

Fig. 14. Travelling speeds of various liquid drops (~50 µL) (a) hexane, (b) kerosene, (c) diesel oil, (d) water and (e) milk on SLIPS. (f) Traveling velocity depicts a negative correlation with the kinematic viscosity of various liquids. Reproduced from ref. [111] with permission from American Chemical Society, Copyright 2016.

ice formation was observed on superhydrophobic coating. Few discrete drop and strip shaped ice began to appear on superhydrophobic coating after 1 h, while an ice layer completely covered the hydrophobic coating and continued to grow. After 3 h, the ice formation was observed on both the coatings. However, some areas were still free from ice formation on superhydrophobic coating, confirming its strong anti-icing ability. Cao *et al.* [66] applied the porous superhydrophobic nanoparticle-polymer composite on satellite dish antenna and aluminum plate and evaluated their anti-icing performance in both laboratory as well as in open environment. The hydrophobic silica nanoparticles mixed in polymer binder (prepared from acrylic polymer and silicone resin) were spray-coated on the substrates, followed by overnight curing at room temperature. The superhydrophobic treated and untreated surfaces were exposed to real-time freezing rain in an open environment (Fig. 15c–f). Untreated aluminum plate was fully covered with significant ice, whereas only traces of ice was found on

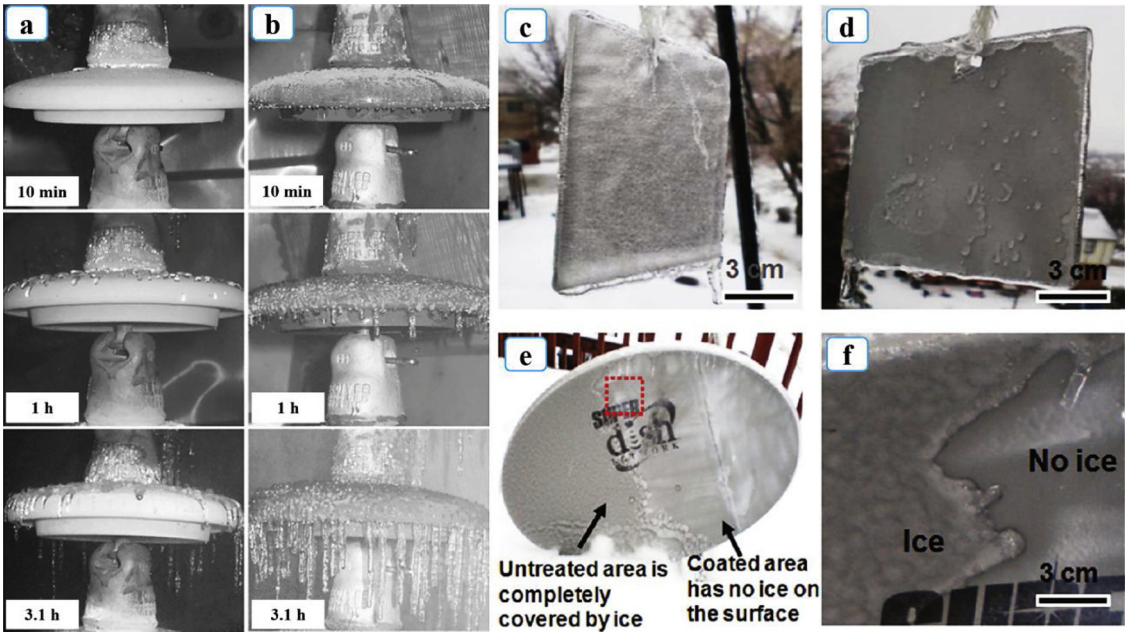

Fig. 15. Evaluation of ice formation on (a) superhydrophobic PDMS/hydrophobic silica nanoparticles coated insulator and (b) RTV silicone rubber coated insulator during different time intervals in laboratory at – 5 °C. Reproduced from ref. [116] with permission from Taylor & Francis, Copyright 2012. Test of anti-icing ability of the surfaces in open environment "freezing rain" (c) bare aluminum plate, (d) superhydrophobic nanocomposite coated aluminum plate, (e) satellite dish antenna. The ice covered on untreated antenna (left side) and no ice accumulation on the superhydrophobic nanocomposite treated antenna (right side), (f) Magnified view of the red square marker in (e), depicting the boundary between the treated (no ice) and untreated area (accumulated ice) of the antenna. Reproduced from ref. [66] with permission from American Chemical Society, Copyright 2009.

superhydrophobic nanocomposite coated aluminum plate (Fig. 15c & d). The same results were observed on treated and untreated parts of a satellite dish antenna in freezing rain conditions, exhibiting practical outdoor application. Untreated portion was fully covered by ice, whereas superhydrophobic nanocomposite treated portion was found to be ice-free (Fig. 15e & f).

Recently, Song et al [117] fabricated durable and inexpensive superhydrophobic concrete coating with excellent anti-icing and anti-corrosion capability which can be of potential use in many civil engineering applications such as roads, bridges, buildings, dams and others. Arshad et al. [118] reviewed the use of superhydrophobic coating in high-voltage outdoor insulation to improve their longevity in adverse environments. They provided the detailed outlook on ice accumulation and prevention on superhydrophobic coatings as well as the performance and mechanical durability of superhydrophobic coating in outdoor use. They also described the electrical performance of the superhydrophobic coating applied on an outdoor insulation. Antonini et al. [119] studied the role of superhydrophobic anti-icing Teflon-coated etched-aluminum surfaces for energy saving applications. The coated substrate can significantly reduce ice formation on the surface due to the repellent and roll-off behavior on the superhydrophobic coating, which, in turn, reduce the heating power required to maintain the wind turbine edges ice-free as compared to the hydrophilic or uncoated surfaces. Recently, Golovin et al. [120] developed low-interfacial toughness (LIT) materials for effective large-scale deicing using polyvinyl chloride (PVC)-, PDMS-, and PS-based coating on an aluminum substrate. These results suggest that icephobic coating can reduce ice adhesion as compared to uncoated substrate. However, at lower icing temperature, an increase in ice adhesion was observed. At the same time, the substrates coated with LIT materials showed complete removal of the adhered ice from the substrate.

Wu et al. [121] prepared a coating material based on a bio-based epoxy resin with excellent transparency on glass substrate as well as on a wooden floor plate and a wood board. Ice accumulation was performed on the bio-based epoxy resin coated and non-coated wooden floor plate and a wood board. The epoxy resin-coated substrates showed an excellent anti-icing character with no residual ice accumulation in contrast to the non-coated substrates where ice accumulation was observed. These results illustrated the good anti-icing performance of the epoxy resin on various substrates. Recently, Huang et al. [122] reviewed briefly about the use of hybrid coating and their anti-icing performance in aerospace applications. Emelyanenko et al. [123] studied the anti-icing performance of the reinforced superhydrophobic coating on silicone rubber. The substrate was fabricated in three steps (i) laser treatment (ii) UV-ozone treatment, (iii) surface treatment by immersing in 1% solution of methoxy-{3-[(2,2,3,3,4,4,5,5,6,6,7,7,8,8,8-pentadecafluorooctyl)-oxy-propyl]-silane in decane for 2 h, and dried for 60 min in an oven at 130 °C. These three-step treatments of silicone rubber exhibited excellent anti-icing performance in severe environmental conditions.

9. Summary

In this review, we briefly described the recent progresses in superhydrophobic anti-icing coating and their uses in a wide range of fields. Anti-icing coating can reduce the energy consumption and increase the productivity of power generation in wind turbines. In aerospace industries, anti-icing coating on the surface of engine and other panels prevents the ice formation and thereby helps to minimize the additional weight of airplanes, resulting in the reduction of fuel consumption. Further, anti-icing coating on the traffic boards, signals, solar panels, and refrigerator systems can reduce energy consumption as well as malfunction of instruments. The icing of water on a superhydrophobic surface depends on several factors such as surface roughness, contact area, temperature and surface thermodynamics. Superhydrophobic coatings can repel water droplets, reduce ice adhesion, and delay ice nucleation which are complementary factors for the anti-icing coatings. However, few materials such as superhydrophobic coatings were not effective in preventing ice formation on the surface at harsh environmental conditions such as heavy snowfall and external mechanical stresses. Therefore, further research is needed for the development of coatings with effective de-icing on any substrates under harsh environment conditions. The drawbacks in superhydrophobic coatings can be overcome by realizing a robust superhydrophobic surface with self-healing or stimuli-responsive superhydrophobic surface property. The capillary condensation of water vapor on the superhydrophobic surface can minimize the anti-icing behavior on the coated substrate, however still posed a challenge on multiple cycles. This can be solved by heating of the superhydrophobic surface to few degrees and also fabricating the substrate with robust texture and chemically stable properties for preventing hydrolysis and condensation of hydrophobic agents. Currently, an emerging research thrust focused on development of highly robust and chemically as well as physically durable superhydrophobic surface for anti-icing applications in harsh environmental conditions. More attention is also needed on the robust slippery superhydrophobic surface (SLIPS) for anti-icing coatings, as the slippery superhydrophobic surface can prevent the ice formation as well as easily drag away the developed ice particles from the surface by simple sliding of the substrate. The introduction of multi-scale cracking such the development of macro-crack initiator with the combination of nano-crack and micro-crack initiators promote the lower ice adhesion on the coated substrates [124]. Another possible approach of anti-icing is the introduction of heating cable which prevent ice development as well as snow accumulation on any substrates. However, the introduction of heat generating material can also have adverse effect on anti-icing performance [125,126]. Recently, heat generating materials gained attentions in anti-icing performance due to easier removal of accumulated ice on the surface. The use of ionic liquids for the anti-icing performance is also reported recently [127]. Likewise, the use phase switching liquid can delay the icing and frost formation [128]. We believe that this review article can give readers deeper insights on the ice formation, and their prevention methods, role of superhydrophobic surface and various development and fabrication pathways of anti-icing coating for different kinds of applications.

Declaration of Competing Interest

The authors declare that there are no conflicts of interest.

Acknowledgements

This work is financially supported by DST – INSPIRE Faculty Scheme, Department of Science and Technology (DST), Govt. of India. [DST/INSPIRE/04/2015/000281]. SSL acknowledges financial assistance from the Henan University, Kaifeng, P. R. China. We greatly appreciate the support of the National Natural Science Foundation of China (21776061) and (21950410531), Foundation of Henan province (182102410090). S. Nagappan and C. S. Ha thanks to the financial support from the National Research Foundation of Korea (NRF) Grant funded by the Ministry of Science and ICT, Korea (NRF2017R1A2B3012961); Brain Korea 21 Plus Program (21A2013800002).

References

[1] V.A. Ganesh, H.K. Raut, A.S. Nair, S. Ramakrishna, A review on self-cleaning coatings, J. Mater. Chem. 21 (41) (2011) 16304–16322.
[2] S. Latthe, C. Terashima, K. Nakata, A. Fujishima, Superhydrophobic surfaces developed by mimicking hierarchical surface morphology of lotus leaf, Molecules 19 (4) (2014) 4256–4283.
[3] L.B. Boinovich, A.M. Emelyanenko, Anti-icing potential of superhydrophobic coatings, Mendeleev Commun. 23 (1) (2013) 3–10.
[4] H. Sojoudi, M. Wang, N. Boscher, G. McKinley, K. Gleason, Durable and scalable

icephobic surfaces: similarities and distinctions from superhydrophobic surfaces, Soft Matter 12 (7) (2016) 1938–1963.
[5] H.J. Ensikat, P. Ditsche-Kuru, C. Neinhuis, W. Barthlott, Superhydrophobicity in perfection: the outstanding properties of the lotus leaf, Beilstein J. Nanotechnol. 2 (2011) 152.
[6] W. Barthlott, C. Neinhuis, Purity of the sacred lotus, or escape from contamination in biological surfaces, Planta 202 (1) (1997) 1–8.
[7] K. Koch, B. Bhushan, W. Barthlott, Multifunctional surface structures of plants: an inspiration for biomimetics, Prog. Mater. Sci. 54 (2) (2009) 137–178.
[8] C. Neinhuis, W. Barthlott, Characterization and distribution of water-repellent, self-cleaning plant surfaces, Ann. Bot. 79 (6) (1997) 667–677.
[9] L. Oberli, D. Caruso, C. Hall, M. Fabretto, P.J. Murphy, D. Evans, Condensation and freezing of droplets on superhydrophobic surfaces, Adv. Colloid Interface Sci. 210 (2014) 47–57.
[10] S.S. Latthe, A.L. Demirel, Polystyrene/octadecyltrichlorosilane superhydrophobic coatings with hierarchical morphology, Polym. Chem. 4 (2) (2013) 246–249.
[11] R.N. Wenzel, Resistance of solid surfaces to wetting by water, Ind. Eng. Chem. 28 (8) (1936) 988–994.
[12] A. Cassie, S. Baxter, Wettability of porous surfaces, Trans. Faraday Soc. 40 (1944) 546–551.
[13] T. Onda, S. Shibuichi, N. Satoh, K. Tsujii, Super-water-repellent fractal surfaces, Langmuir 12 (9) (1996) 2125–2127.
[14] S. Liu, S.S. Latthe, H. Yang, B. Liu, R. Xing, Raspberry-like superhydrophobic silica coatings with self-cleaning properties, Ceram. Int. 41 (9, Part B) (2015) 11719–11725.
[15] S.S. Latthe, K. Nakata, R. Höfer, A. Fujishima, C. Terashima, Lotus effect-based superhydrophobic surfaces: candle soot as a promising class of nanoparticles for self-cleaning and oil–water separation applications, Green Chemistry for Surface Coatings, Inks and Adhesives, (2019), pp. 92–119.
[16] S.S. Latthe, R.S. Sutar, V.S. Kodag, A.K. Bhosale, A.M. Kumar, K. Kumar Sadasivuni, R. Xing, S. Liu, Self – cleaning superhydrophobic coatings: potential industrial applications, Prog. Org. Coat. 128 (2019) 52–58.
[17] R. Xing, S.S. Latthe, A.K. Bhosale, R. Li, A. Madhan Kumar, S. Liu, A novel and facile approach to prepare self-cleaning yellow superhydrophobic polycarbonates, J. Mol. Liq. 247 (2017) 366–373.
[18] S. Liu, X. Liu, S.S. Latthe, L. Gao, S. An, S.S. Yoon, B. Liu, R. Xing, Self-cleaning transparent superhydrophobic coatings through simple sol–gel processing of fluoroalkylsilane, Appl. Surf. Sci. 351 (2015) 897–903.
[19] Y. Si, Z. Dong, L. Jiang, Bioinspired designs of superhydrophobic and superhydrophilic materials, ACS Cent. Sci. 4 (9) (2018) 1102–1112.
[20] M. Ruan, W. Li, B. Wang, B. Deng, F. Ma, Z. Yu, Preparation and anti-icing behavior of superhydrophobic surfaces on aluminum alloy substrates, Langmuir 29 (27) (2013) 8482–8491.
[21] X. Wu, V.V. Silberschmidt, Z.-T. Hu, Z. Chen, When superhydrophobic coatings are icephobic: role of surface topology, Surf. Coat. Technol. 358 (2019) 207–214.
[22] H.J. Ensikat, A.J. Schulte, K. Koch, W. Barthlott, Droplets on superhydrophobic surfaces: visualization of the contact area by cryo-scanning electron microscopy, Langmuir 25 (22) (2009) 13077–13083.
[23] M. Nosonovsky, V. Hejazi, Why superhydrophobic surfaces are not always icephobic, ACS Nano 6 (10) (2012) 8488–8491.
[24] L. Wang, Q. Gong, S. Zhan, L. Jiang, Y. Zheng, Robust anti-icing performance of a flexible superhydrophobic surface, Adv. Mater. 28 (35) (2016) 7729–7735.
[25] Q. Liu, Y. Yang, M. Huang, Y. Zhou, Y. Liu, X. Liang, Durability of a lubricant-infused electrospray silicon rubber surface as an anti-icing coating, Appl. Surf. Sci. 346 (2015) 68–76.
[26] Z. Zuo, R. Liao, C. Guo, X. Zhao, A. Zhuang, Y. Yuan, Fabrication of self-cleaning and anti-icing durable surface on glass, J. Nanosci. Nanotechnol. 17 (1) (2017) 420–426.
[27] L.B. Boinovich, A.M. Emelyanenko, Anti-icing potential of superhydrophobic coatings, Mendeleev Commun. 1 (23) (2013) 3–10.
[28] J. Lv, Y. Song, L. Jiang, J. Wang, Bio-inspired strategies for anti-icing, ACS Nano 8 (4) (2014) 3152–3169.
[29] M.J. Kreder, J. Alvarenga, P. Kim, J. Aizenberg, Design of anti-icing surfaces: smooth, textured or slippery? Nat. Rev. Mater. 1 (1) (2016) 15003.
[30] S. Zhang, J. Huang, Y. Cheng, H. Yang, Z. Chen, Y. Lai, Bioinspired surfaces with superwettability for anti-icing and ice-phobic application: concept, mechanism, and design, Small 13 (48) (2017) 1701867.
[31] M. Liu, S. Wang, L. Jiang, Nature-inspired superwettability systems, Nat. Rev. Mater. 2 (7) (2017) 17036.
[32] Y. Liu, D. Song, C.-H. Choi, Anti-and de-icing behaviors of superhydrophobic fabrics, Coatings 8 (6) (2018) 198.
[33] Q. Li, Z. Guo, Fundamentals of icing and common strategies for designing biomimetic anti-icing surfaces, J. Mater. Chem. A 6 (28) (2018) 13549–13581.
[34] S. Jin, J. Liu, J. Lv, S. Wu, J. Wang, Interfacial materials for anti-icing: beyond superhydrophobic surfaces, Chem.–Asian J. 13 (11) (2018) 1406–1414.
[35] Y. Lin, H. Chen, G. Wang, A. Liu, Recent progress in preparation and anti-icing applications of superhydrophobic coatings, Coatings 8 (6) (2018) 208.
[36] Y. Shen, X. Wu, J. Tao, C. Zhu, Y. Lai, Z. Chen, Icephobic materials: fundamentals, performance evaluation, and applications, Prog. Mater. Sci. 103 (2019) 509–557.
[37] X. Sun, V.G. Damle, S. Liu, K. Rykaczewski, Bioinspired stimuli-responsive and antifreeze-secreting anti-icing coatings, Adv. Mater. Interfaces 2 (5) (2015) 1400479.
[38] S.E. Chang, T.L. McDaniels, J. Mikawoz, K. Peterson, Infrastructure failure interdependencies in extreme events: power outage consequences in the 1998 Ice Storm, Nat. Hazards 41 (2) (2007) 337–358.
[39] W. Zhou, J.C. Chan, W. Chen, J. Ling, J.G. Pinto, Y. Shao, Synoptic-scale controls of persistent low temperature and icy weather over southern China in January 2008, Mon. Weather. Rev. 137 (11) (2009) 3978–3991.
[40] R. Carriveau, A. Edrisy, P. Cadieux, R. Mailloux, Ice adhesion issues in renewable energy infrastructure, J. Adhes. Sci. Technol. 26 (4-5) (2012) 447–461.
[41] O. Parent, A. Ilinca, Anti-icing and de-icing techniques for wind turbines: critical review, Cold Reg. Sci. Technol. 65 (1) (2011) 88–96.
[42] R. Gent, N. Dart, J. Cansdale, Aircraft icing, Philos. Trans. R. Soc. Lond. A: Math. Phys. Eng. Sci. 358 (1776) (2000) 2873–2911.
[43] C.C. Ryerson, Assessment of Superstructure Ice Protection As Applied to Offshore Oil Operations Safety, (2009).
[44] V. Bahadur, L. Mishchenko, B. Hatton, J.A. Taylor, J. Aizenberg, T. Krupenkin, Predictive model for ice formation on superhydrophobic surfaces, Langmuir 27 (23) (2011) 14143–14150.
[45] B.P. Jelle, The challenge of removing snow downfall on photovoltaic solar cell roofs in order to maximize solar energy efficiency—research opportunities for the future, Energy Build. 67 (2013) 334–351.
[46] J. Laforte, M. Allaire, J. Laflamme, State-of-the-art on power line de-icing, Atmos. Res. 46 (1) (1998) 143–158.
[47] C. Machielsen, H. Kerschbaumer, Influence of frost formation and defrosting on the performance of air coolers: standards and dimensionless coefficients for the system designer, Int. J. Refrig. 12 (5) (1989) 283–290.
[48] D. Byun, J. Hong, J.H. Ko, Y.J. Lee, H.C. Park, B.-K. Byun, J.R. Lukes, Wetting characteristics of insect wing surfaces, J. Bionic Eng. 6 (1) (2009) 63–70.
[49] S. Wang, Z. Yang, G. Gong, J. Wang, J. Wu, S. Yang, L. Jiang, Icephobicity of Penguins Spheniscus humboldti and an artificial replica of penguin feather with air-infused hierarchical rough structures, J. Phys. Chem. C 120 (29) (2016) 15923–15929.
[50] H.F. Bohn, W. Federle, Insect aquaplaning: *Nepenthes* pitcher plants capture prey with the peristome, a fully wettable water-lubricated anisotropic surface, Proc. Natl. Acad. Sci. U. S. A. 101 (39) (2004) 14138–14143.
[51] T.-S. Wong, S.H. Kang, S.K.Y. Tang, E.J. Smythe, B.D. Hatton, A. Grinthal, J. Aizenberg, Bioinspired self-repairing slippery surfaces with pressure-stable omniphobicity, Nature 477 (2011) 443.
[52] P. Kim, T.-S. Wong, J. Alvarenga, M.J. Kreder, W.E. Adorno-Martinez, J. Aizenberg, Liquid-infused nanostructured surfaces with extreme anti-ice and anti-frost performance, ACS Nano 6 (8) (2012) 6569–6577.
[53] P.W. Wilson, W. Lu, H. Xu, P. Kim, M.J. Kreder, J. Alvarenga, J. Aizenberg, Inhibition of ice nucleation by slippery liquid-infused porous surfaces (SLIPS), J. Chem. Soc. Faraday Trans. 15 (2) (2013) 581–585.
[54] T.-S. Wong, S.H. Kang, S.K. Tang, E.J. Smythe, B.D. Hatton, A. Grinthal, J. Aizenberg, Bioinspired self-repairing slippery surfaces with pressure-stable omniphobicity, Nature 477 (7365) (2011) 443–447.
[55] H. Saito, K. Takai, G. Yamauchi, Water-and ice-repellent coatings, Surf. Coat. Int. Part B Coat. Trans. 80 (4) (1997) 168–171.
[56] H. Koivuluoto, C. Stenroos, M. Kylmälahti, M. Apostol, J. Kiilakoski, P. Vuoristo, Anti-icing behavior of thermally sprayed polymer coatings, J. Therm. Spray Technol. 26 (1) (2017) 150–160.
[57] R. Dou, J. Chen, Y. Zhang, X. Wang, D. Cui, Y. Song, L. Jiang, J. Wang, Anti-icing coating with an aqueous lubricating layer, ACS Appl. Mater. Interfaces 6 (10) (2014) 6998–7003.
[58] K. Xu, J. Hu, X. Jiang, W. Meng, B. Lan, L. Shu, Anti-icing performance of hydrophobic silicone–acrylate resin coatings on wind blades, Coatings 8 (4) (2018) 151.
[59] P. Guo, Y. Zheng, M. Wen, C. Song, Y. Lin, L. Jiang, Icephobic/anti-icing properties of micro/nanostructured surfaces, Adv. Mater. 24 (19) (2012) 2642–2648.
[60] T.-B. Nguyen, S. Park, H. Lim, Effects of morphology parameters on anti-icing performance in superhydrophobic surfaces, Appl. Surf. Sci. 435 (2018) 585–591.
[61] S. Rajiv, S. Kumaran, M. Sathish, Long-term-durable anti-icing superhydrophobic composite coatings, J. Appl. Polym. Sci. 136 (7) (2019) 47059.
[62] W. Peng, X. Gou, H. Qin, M. Zhao, X. Zhao, Z. Guo, Creation of a multifunctional superhydrophobic coating for composite insulators, Chem. Eng. J. 352 (2018) 774–781.
[63] A. Alizadeh, M. Yamada, R. Li, W. Shang, S. Otta, S. Zhong, L. Ge, A. Dhinojwala, K.R. Conway, V. Bahadur, Dynamics of ice nucleation on water repellent surfaces, Langmuir 28 (6) (2012) 3180–3186.
[64] L.B. Boinovich, A.M. Emelyanenko, V.K. Ivanov, A.S. Pashinin, Durable icephobic coating for stainless steel, ACS Appl. Mater. Interfaces 5 (7) (2013) 2549–2554.
[65] L. Mishchenko, B. Hatton, V. Bahadur, J.A. Taylor, T. Krupenkin, J. Aizenberg, Design of ice-free nanostructured surfaces based on repulsion of impacting water droplets, ACS Nano 4 (12) (2010) 7699–7707.
[66] L. Cao, A.K. Jones, V.K. Sikka, J. Wu, D. Gao, Anti-icing superhydrophobic coatings, Langmuir 25 (21) (2009) 12444–12448.
[67] J. Chen, J. Liu, M. He, K. Li, D. Cui, Q. Zhang, X. Zeng, Y. Zhang, J. Wang, Y. Song, Superhydrophobic surfaces cannot reduce ice adhesion, Appl. Phys. Lett. 101 (11) (2012) 111603.
[68] K.K. Varanasi, T. Deng, J.D. Smith, M. Hsu, N. Bhate, Frost formation and ice adhesion on superhydrophobic surfaces, Appl. Phys. Lett. 97 (23) (2010) 234102.
[69] T. Bharathidasan, S.V. Kumar, M.S. Bobji, R.P.S. Chakradhar, B.J. Basu, Effect of wettability and surface roughness on ice-adhesion strength of hydrophilic, hydrophobic and superhydrophobic surfaces, Appl. Surf. Sci. 314 (2014) 241–250.
[70] T.-B. Nguyen, S. Park, Y. Jung, H. Lim, Effects of hydrophobicity and lubricant characteristics on anti-icing performance of slippery lubricant-infused porous surfaces, J. Ind. Eng. Chem. 69 (2019) 99–105.
[71] L. Zhu, J. Xue, Y. Wang, Q. Chen, J. Ding, Q. Wang, Ice-phobic coatings based on silicon-oil-infused polydimethylsiloxane, ACS Appl. Mater. Interfaces 5 (10) (2013) 4053–4062.

[72] J. Zhang, C. Gu, J. Tu, Robust slippery coating with superior corrosion resistance and anti-icing performance for AZ31B Mg alloy protection, ACS Appl. Mater. Interfaces 9 (12) (2017) 11247–11257.
[73] T. Yu, S. Lu, W. Xu, R. Boukherroub, Preparation of superhydrophobic/superoleophilic copper coated titanium mesh with excellent ice-phobic and water-oil separation performance, Appl. Surf. Sci. 476 (2019) 353–362.
[74] N. Hassan, S. Lu, W. Xu, G. He, M. Faheem, N. Ahmad, M.A. Khan, B.Z. Butt, Fabrication of a Pt nanoparticle surface on an aluminum substrate to achieve excellent superhydrophobicity and catalytic activity, New J. Chem. 43 (15) (2019) 6069–6079.
[75] Z. Zuo, X. Song, R. Liao, X. Zhao, Y. Yuan, Understanding the anti-icing property of nanostructured superhydrophobic aluminum surface during glaze ice accretion, Int. J. Heat Mass Transf. 133 (2019) 119–128.
[76] E.J.Y. Ling, V. Uong, J.-Sb. Renault-Crispo, A.-M. Kietzig, P. Servio, Reducing ice adhesion on nonsmooth metallic surfaces: wettability and topography effects, ACS Appl. Mater. Interfaces 8 (13) (2016) 8789–8800.
[77] S.F. Ahmadi, S. Nath, G.J. Iliff, B.R. Srijanto, C.P. Collier, P. Yue, J.B. Boreyko, Passive antifrosting surfaces using microscopic ice patterns, ACS Appl. Mater. Interfaces 10 (38) (2018) 32874–32884.
[78] D. Choi, J. Yoo, S.M. Park, D.S. Kim, Facile and cost-effective fabrication of paternable superhydrophobic surfaces via salt dissolution assisted etching, Appl. Surf. Sci. 393 (2017) 449–456.
[79] N. Wang, D. Xiong, Y. Deng, Y. Shi, K. Wang, Mechanically robust superhydrophobic steel surface with anti-icing, UV-durability, and corrosion resistance properties, ACS Appl. Mater. Interfaces 7 (11) (2015) 6260–6272.
[80] S. Zheng, C. Li, Q. Fu, T. Xiang, W. Hu, J. Wang, S. Ding, P. Liu, Z. Chen, Fabrication of a micro-nanostructured superhydrophobic aluminum surface with excellent corrosion resistance and anti-icing performance, RSC Adv. 6 (83) (2016) 79389–79400.
[81] Q. Hao, Y. Pang, Y. Zhao, J. Zhang, J. Feng, S. Yao, Mechanism of delayed frost growth on superhydrophobic surfaces with jumping condensates: more than interdrop freezing, Langmuir 30 (51) (2014) 15416–15422.
[82] K. Li, S. Xu, W. Shi, M. He, H. Li, S. Li, X. Zhou, J. Wang, Y. Song, Investigating the effects of solid surfaces on ice nucleation, Langmuir 28 (29) (2012) 10749–10754.
[83] H. Wang, G. He, Q. Tian, Effects of nano-fluorocarbon coating on icing, Appl. Surf. Sci. 258 (18) (2012) 7219–7224.
[84] N. Wang, D. Xiong, M. Li, Y. Deng, Y. Shi, K. Wang, Superhydrophobic surface on steel substrate and its anti-icing property in condensing conditions, Appl. Surf. Sci. 355 (2015) 226–232.
[85] Y. Cheng, S. Lu, W. Xu, Controllable wettability of micro-and nano-dendritic structures formed on aluminum substrates, New J. Chem. 39 (8) (2015) 6602–6610.
[86] Z. Yuan, J. Bin, X. Wang, Q. Liu, D. Zhao, H. Chen, H. Jiang, Preparation and anti-icing property of a lotus-leaf-like superhydrophobic low-density polyethylene coating with low sliding angle, Polym. Eng. Sci. 52 (11) (2012) 2310–2315.
[87] S. Hong, R. Wang, X. Huang, H. Liu, Facile one-step fabrication of PHC/PDMS anti-icing coatings with mechanical properties and good durability, Prog. Org. Coat. 135 (2019) 263–269.
[88] Q. Yang, Z. Luo, F. Jiang, Y. Luo, S. Tan, Z. Lu, Z. Zhang, W. Liu, Air cushion convection inhibiting icing of self-cleaning surfaces, ACS Appl. Mater. Interfaces 8 (42) (2016) 29169–29178.
[89] C. Li, X. Li, C. Tao, L. Ren, Y. Zhao, S. Bai, X. Yuan, Amphiphilic antifogging/anti-icing coatings containing POSS-PDMAEMA-b-PSBMA, ACS Appl. Mater. Interfaces 9 (27) (2017) 22959–22969.
[90] H. Koivuluoto, C. Stenroos, M. Kylmälahti, M. Apostol, J. Kiilakoski, P. Vuoristo, Anti-icing behavior of thermally sprayed polymer coatings, J. Therm. Spray Technol. 26 (1-2) (2017) 150–160.
[91] Y.-H. Ng, S.-W. Tay, L. Hong, Formation of icephobic surface with micron-scaled hydrophobic heterogeneity on polyurethane aerospace coating, ACS Appl. Mater. Interfaces 10 (43) (2018) 37517–37528.
[92] Z. He, E.T. Vågenes, C. Delabahan, J. He, Z. Zhang, Room temperature characteristics of polymer-based low ice adhesion surfaces, Sci. Rep. 7 (2017) 42181.
[93] K.D. Esmeryan, A.H. Bressler, C.E. Castano, C.P. Fergusson, R. Mohammadi, Rational strategy for the atmospheric icing prevention based on chemically functionalized carbon soot coatings, Appl. Surf. Sci. 390 (2016) 452–460.
[94] Y. Zhang, M.R. Klittich, M. Gao, A. Dhinojwala, Delaying frost formation by controlling surface chemistry of carbon nanotube-coated steel surfaces, ACS Appl. Mater. Interfaces 9 (7) (2017) 6512–6519.
[95] S. Pan, N. Wang, D. Xiong, Y. Deng, Y. Shi, Fabrication of superhydrophobic coating via spraying method and its applications in anti-icing and anti-corrosion, Appl. Surf. Sci. 389 (2016) 547–553.
[96] J. Liu, Z.A. Janjua, M. Roe, F. Xu, B. Turnbull, K.-S. Choi, X. Hou, Super-hydrophobic/icephobic coatings based on silica nanoparticles modified by self-assembled monolayers, Nanomaterials 6 (12) (2016) 232.
[97] X. Zhan, Y. Yan, Q. Zhang, F. Chen, A novel superhydrophobic hybrid nanocomposite material prepared by surface-initiated AGET ATRP and its anti-icing properties, J. Mater. Chem. A 2 (24) (2014) 9390–9399.
[98] Q. Shang, Y. Zhou, Fabrication of transparent superhydrophobic porous silica coating for self-cleaning and anti-fogging, Ceram. Int. 42 (7) (2016) 8706–8712.
[99] E.B. Caldona, A.C.C. De Leon, P.G. Thomas, D.F. Naylor, B.B. Pajarito, R.C. Advincula, Superhydrophobic rubber-modified polybenzoxazine/SiO2 nanocomposite coating with anticorrosion, anti-ice, and superoleophilicity properties, Ind. Eng. Chem. Res. 56 (6) (2017) 1485–1497.
[100] X. Wu, Z. Chen, A mechanically robust transparent coating for anti-icing and self-cleaning applications, J. Mater. Chem. A 6 (33) (2018) 16043–16052.
[101] Y. Li, B. Li, X. Zhao, N. Tian, J. Zhang, Totally waterborne, nonfluorinated, mechanically robust, and self-healing superhydrophobic coatings for actual anti-icing, ACS Appl. Mater. Interfaces 10 (45) (2018) 39391–39399.
[102] G. Momen, R. Jafari, M. Farzaneh, Ice repellency behaviour of superhydrophobic surfaces: effects of atmospheric icing conditions and surface roughness, Appl. Surf. Sci. 349 (2015) 211–218.
[103] L. Wang, M. Wen, M. Zhang, L. Jiang, Y. Zheng, Ice-phobic gummed tape with nano-cones on microspheres, J. Mater. Chem. A 2 (10) (2014) 3312–3316.
[104] C. Yang, F. Wang, W. Li, J. Ou, C. Li, A. Amirfazli, Anti-icing properties of superhydrophobic ZnO/PDMS composite coating, Appl. Phys. A 122 (1) (2016) 1.
[105] S.-P. Fu, R.P. Sahu, E. Diaz, J.R. Robles, C. Chen, X. Rui, R.F. Klie, A.L. Yarin, J.T. Abiade, Dynamic study of liquid drop impact on supercooled cerium dioxide: anti-icing behavior, Langmuir 32 (24) (2016) 6148–6162.
[106] W. Tong, D. Xiong, N. Wang, C. Yan, T. Tian, Green and timesaving fabrication of a superhydrophobic surface and its application to anti-icing, self-cleaning and oil-water separation, Surf. Coat. Technol. 352 (2018) 609–618.
[107] S. Nagappan, N.-J. Jo, W.-K. Lee, C.-S. Ha, Thermally stable superhydrophobic polymethylhydrosiloxane nanohybrids with liquid marble-like structure, Macromol. Res. 25 (5) (2017) 387–390.
[108] A. Hashmi, A. Strauss, J. Xu, Freezing of a liquid marble, Langmuir 28 (28) (2012) 10324–10328.
[109] D. Zang, K. Lin, W. Wang, Y. Gu, Y. Zhang, X. Geng, B.P. Binks, Tunable shape transformation of freezing liquid water marbles, Soft Matter 10 (9) (2014) 1309–1314.
[110] N. Wang, D. Xiong, S. Pan, K. Wang, Y. Shi, Y. Deng, Robust superhydrophobic coating and the anti-icing properties of its lubricants-infused-composite surface under condensing condition, New J. Chem. 41 (4) (2017) 1846–1853.
[111] N. Wang, D. Xiong, Y. Lu, S. Pan, K. Wang, Y. Deng, Y. Shi, Design and fabrication of the lyophobic slippery surface and its application in anti-icing, J. Phys. Chem. C 120 (20) (2016) 11054–11059.
[112] M. Liu, Y. Hou, J. Li, L. Tie, Z. Guo, Transparent slippery liquid-infused nanoparticulate coatings, Chem. Eng. J. 337 (2018) 462–470.
[113] M. Cao, D. Guo, C. Yu, K. Li, M. Liu, L. Jiang, Water-repellent properties of superhydrophobic and lubricant-infused "slippery" surfaces: a brief study on the functions and applications, ACS Appl. Mater. Interfaces 8 (6) (2015) 3615–3623.
[114] G. Zhang, Q. Zhang, T. Cheng, X. Zhan, F. Chen, Polyols-infused slippery surfaces based on magnetic Fe3O4-Functionalized polymer hybrids for enhanced multifunctional anti-icing and deicing properties, Langmuir 34 (13) (2018) 4052–4058.
[115] C. Peng, S. Xing, Z. Yuan, J. Xiao, C. Wang, J. Zeng, Preparation and anti-icing of superhydrophobic PVDF coating on a wind turbine blade, Appl. Surf. Sci. 259 (2012) 764–768.
[116] J. Li, Y. Zhao, J. Hu, L. Shu, X. Shi, Anti-icing performance of a superhydrophobic PDMS/modified nano-silica hybrid coating for insulators, J. Adhes. Sci. Technol. 26 (4-5) (2012) 665–679.
[117] J. Song, Y. Li, W. Xu, H. Liu, Y. Lu, Inexpensive and non-fluorinated superhydrophobic concrete coating for anti-icing and anti-corrosion, J. Colloid Interface Sci. 541 (2019) 86–92.
[118] G. Momen, M. Farzaneh, A. Nekahi, Properties and applications of superhydrophobic coatings in high voltage outdoor insulation: a review, Ieee Trans. Dielectr. Electr. Insul. 24 (6) (2017) 3630–3646.
[119] C. Antonini, M. Innocenti, T. Horn, M. Marengo, A. Amirfazli, Understanding the effect of superhydrophobic coatings on energy reduction in anti-icing systems, Cold Reg. Sci. Technol. 67 (1-2) (2011) 58–67.
[120] K. Golovin, A. Dhyani, M. Thouless, A. Tuteja, Low–interfacial toughness materials for effective large-scale deicing, Science 364 (6438) (2019) 371–375.
[121] X. Wu, S. Zheng, D.A. Bellido-Aguilar, V.V. Silberschmidt, Z. Chen, Transparent icephobic coatings using bio-based epoxy resin, Mater. Des. 140 (2018) 516–523.
[122] X. Huang, N. Tepylo, V. Pommier-Budinger, M. Budinger, E. Bonaccurso, P. Villedieu, L. Bennani, A survey of icephobic coatings and their potential use in a hybrid coating/active ice protection system for aerospace applications, Prog. Aerosp. Sci. 105 (2019) 74–97.
[123] A.M. Emelyanenko, L.B. Boinovich, A.A. Bezdomnikov, E.V. Chulkova, K.A. Emelyanenko, Reinforced superhydrophobic coating on silicone rubber for longstanding anti-icing performance in severe conditions, ACS Appl. Mater. Interfaces 9 (28) (2017) 24210–24219.
[124] Z. He, S. Xiao, H. Gao, J. He, Z. Zhang, Multiscale crack initiator promoted superlow ice adhesion surfaces, Soft Matter 13 (37) (2017) 6562–6568.
[125] L. Vertuccio, F. De Santis, R. Pantani, K. Lafdi, L. Guadagno, Effective de-icing skin using graphene-based flexible heater, Compos. Part B Eng. 162 (2019) 600–610.
[126] N. Karim, M. Zhang, S. Afroj, V. Koncherry, P. Potluri, K.S. Novoselov, Graphene-based surface heater for de-icing applications, RSC Adv. 8 (30) (2018) 16815–16823.
[127] R. Chatterjee, D. Beysens, S. Anand, Delaying ice and frost formation using phase-switching liquids, Adv. Mater. 31 (17) (2019) 1807812.
[128] D. Aydin, M.B. Akolpoglu, R. Kizilel, S. Kizilel, Anti-icing properties on surfaces through a functional composite: effect of ionic salts, ACS Omega 3 (7) (2018) 7934–7943.